Tunable Compact Microwave Multiplexers based on Substrate Integrated Waveguide

by

Mohammad Dawodi

A thesis submitted to the
School of Graduate and Postdoctoral Studies in partial
fulfillment of the requirements for the degree of

Master of Applied Science in Electrical and Computer Engineering

The Faculty of Engineering and Applied Science

University of Ontario Institute of Technology (Ontario Tech University)

Oshawa, Ontario, Canada

May 2021

THESIS EXAMINATION INFORMATION

Submitted by: **Mohammad Dawodi**

Master of Applied Science
in
Electrical and Computer Engineering

Thesis title: Tunable Compact Microwave Multiplexers based on Substrate Integrated Waveguide

An oral defense of this thesis took place on May 19th, 2021 in front of the following examining committee:

Examining Committee:

Chair of Examining Committee	Dr. Jing Ren
Research Supervisor	Dr. Ying Wang
Research Co-supervisor	Dr. Ming Yu
Examining Committee Member	Dr. Farhan Abdul Ghaffar
Thesis Examiner	Dr. Ruth Milman

The above committee determined that the thesis is acceptable in form and content and that a satisfactory knowledge of the field covered by the thesis was demonstrated by the candidate during an oral examination. A signed copy of the Certificate of Approval is available from the School of Graduate and Postdoctoral Studies.

ABSTRACT

Microwave multiplexers and diplexers are widely used in communication systems. This thesis presents a compact low-profile hybrid-coupled filter module (HCFM) implemented using substrate integrated waveguide (SIW). Compared to conventional rectangular waveguide HCFM, the new design achieves 60% reduction in size. The feasibility of electronic tuning of the HCFM is also investigated using full wave electromagnetic (EM) simulations. The compact SIW HCFM is further validated using measurement results. Good agreement between simulation and measurement results is achieved.

In addition, a new method is proposed for implementing tunable diplexers. The tunable diplexer is formed by cascading a bandpass filter with the HCFM, thereby simplifying the tuning complexity of diplexers. Particularly, the bandwidths and center frequencies of the diplexer can be modified by simply tuning the center frequencies of the bandpass filters and/or the HCFM. Tunability of the diplexer is investigated considering different scenarios. Moreover, the concept is validated through measurement results.

Keywords: hybrid-coupled filter module; microwave filters; microwave multiplexer; tunable diplexer

AUTHOR'S DECLARATION

I hereby declare that this thesis consists of original work of which I have authored. This is a true copy of the thesis, including any required final revisions, as accepted by my examiners.

I authorize the Ontario Tech University to lend this thesis to other institutions or individuals for the purpose of scholarly research. I further authorize Ontario Tech University to reproduce this thesis by photocopying or by other means, in total or in part, at the request of other institutions or individuals for the purpose of scholarly research. I understand that my thesis will be made electronically available to the public.

Mohammad Dawodi

STATEMENT OF CONTRIBUTIONS

The work described in Chapter 4 will be submitted for publication as:

M. Dawodi, Y. Wang, and M. Yu, “Tunable Diplexer based on Hybrid-coupled Filter Module (HCFM)," *2021International Microwave Filter Workshop (IMFW)*, Nov. 2021 [To be submitted].

I performed the majority of the simulation, and measurements.

ACKNOWLEDGEMENTS

Throughout the course of my master degree, I have received a great deal of support and assistance. I would first like to thank my supervisor, Dr. Ying Wang and my co-supervisor Dr. Ming Yu for all their supports and encouragements. My special thanks to professor Wang. Your insightful feedback pushed me to sharpen my thinking and brought my work to a higher level.

I would also like to thank my friends and colleagues for their kind and endless supports. In addition, I would like to thank my parents for their wise counsel and sympathetic ear. You are always there for me. Finally, I could not have completed this dissertation without the support and help of my wife Sharifa Kakar.

Mohammad Dawodi

Oshawa, Ontario

Lovingly dedicated to

My lovely wife **Sharifa**

And to our beautiful children, **Hoda**, **Elias**, **Edris**, **Ebrahim**, and **Sedra**

You are the light and inspiration of my LIFE

TABLE OF CONTENTS

LIST OF TABLES

LIST OF FIGURES

LIST OF ABBREVIATIONS

ADS	Advance Design System
BPF	Bandpass Filter
CPW	Coplanar Waveguide
DFW	Dielectric Filled Rectangular Waveguide
EM	Electromagnetic
HCFM	Hybrid-Coupled Filter Module
HFSS	High-Frequency Structure Simulator
MEMS	Micro-Electro-Mechanical Systems
SICs	Substrate Integrated Circuits
SIW	Substrate Integrated Waveguide

Chapter 1

Introduction

1.1 Overview

In this era of rapid growing technology, the field of microwave communication system is moving towards miniaturization of components, lowering the manufacturing cost, and improving functionality of the system. Microwave multiplexers and diplexers are widely used in communication systems as combiners and channelizers [1]. Compactness, low cost, and tunability are highly desirable characteristics.

Radio frequency (RF) and microwave circuits, can be implemented in different technologies, including non-planar circuits, for example rectangular waveguides, and planar circuits, for example microstrip or coplanar waveguide (CPW). Multiplexers and diplexers using rectangular waveguide, with high power handling capability and high quality (Q) factor, i.e. low loss, are still one of the most reliable solutions for many applications. However, in addition to its bulkiness, the integration of waveguides with planar circuits can be challenging. On the other hand, conventional planar circuits are typically compact, easy to fabricate and to integrate, and low cost. However, the loss is usually high. Substrate integrated circuits (SICs), such as substrate integrated waveguide (SIW), are relatively new technologies and have attract much attention for various applications. Comparing to non-planar circuits, SIW technology offers great benefit on size reduction, ease of fabrication, low cost, and the simplicity of integration with other planar

circuits. At the same time, it has improved loss performance comparing to conventional planar circuits.

1.2 Motivations

There are different configurations for microwave multiplexers. A hybrid coupled multiplexer is formed by using a number of hybrid-coupled filter modules (HCFMs), and is one of the most commonly used configurations. A conventional HCFM multiplexer's size is larger than other types of multiplexer because each channel requires two identical filters and two hybrids. A more compact HCFM multiplexer using rectangular waveguide was presented in [2]. Despite of its reduced size, the improved design still suffers from the disadvantages associated with rectangular waveguides.

In this thesis, we investigate the implementation of the improved HCFM using SIW technology. In addition to its compactness, the SIW allows additional flexibility in the layout and waveguide design variables. This enables further reduction in the footprint. As will be shown, the distance between two filters can be reduced to almost zero in the new topology of the SIW HCFM in this thesis.

Tunable microwave circuits, including tunable filters and multiplexers, have attracted a lot of attentions because of the added agility to a communication system. Most research focuses on tunable filters. Tuning multiplexer is more challenging comparing to tuning a standalone filter, due to the interaction among channel filters. One of the advantages of HCFM multiplexers is the fact that there is no interaction between channel filters. It is therefore beneficial to investigate the tunability of the developed HCFM, since combination of tunable HCFMs can lead to tunable multiplexers.

1.3 Thesis Contributions

In this thesis, a compact HCFM implemented using SIW technology is successfully developed and tested. Taking advantage of the compactness and flexibility offered by SIW, the new design achieves 60% footprint reduction comparing to the HCFM previously designed using rectangular waveguide. The electronic tunability of a single cavity resonator and the improved SIW HCFM using varactor diodes is also investigated, and results are supported by full wave electromagnetic (EM) simulations. In addition, the compact HCFM using SIW is validated using measurement results. There is good agreement between EM simulation and measurement results for the designed HCFM.

Furthermore, this thesis presents a novel methodology for implementing tunable diplexers, by simply cascading an SIW bandpass filter with the developed HCFM. This technique reduces the complexity of tuning a diplexer to as simple as tuning a bandpass filter. Simulations of different scenarios show that the bandwidths and center frequencies of the diplexer can be modified by simply tuning the center frequencies of the bandpass filter and/or the HCFM. The concept is also validated through measurement results. Two diplexers are fabricated with only the center frequencies of the bandpass filters being different. The HCFM remains the same in the two cascaded designs. Results show two diplexers with different center frequencies and bandwidths for each channel. Good agreements are shown between EM simulations and measurements for both designs.

1.4 Outline

In Chapter 1, the overview and motivation of the research, thesis contributions, and outline are presented.

Chapter 2 reviews the most recent research on the microwave multiplexers and diplexers, and SIW, along with its design principals. Furthermore, studies on tunable microwave filters and multiplexers are reviewed.

In Chapter 3, the design process of the SIW-based compact HCFM is given in detail. Simulations based on both circuit model and EM models are presented. The feasibility of electronic tuning of the HCFM is also investigated in this chapter. EM simulations are used to demonstrate the tuning range of both SIW cavities and the complete HCFM. In addition, measurement results are presented, validating the compact SIW-based HCFM design.

In Chapter 4, the novel method of realizing a tunable compact microwave diplexer is presented. The diplexer comprises of a bandpass filter and the HCFM developed in Chapter 3. It is demonstrated that the resulted diplexer can be readily tuned by adjusting the bandpass filter and/or the HCFM. Different scenarios are analysed and simulation results are presented. Measurement results are then presented to prove the concept.

Finally, conclusions are drawn in Chapter 5. Suggestions on future research are also provided.

Chapter 2

Literature Review

2.1 Microwave Multiplexers (MUX) and Diplexers

Multiplexers have been employed by communication networks since mid-1970s [2]. They are used as channelizers or combiners. Channelizers in communication systems are needed to separate a single wide band channel into a number of narrow band channels, while combiners are used to combine narrow band channels into a single wide band channel, to be connected to a single antenna. In particular, diplexers are a form of multiplexer that is configured to separate transmit and receive bands in a common device. A typical diplexer structure, as shown in Figure 2-1, includes two distinct filter channels, located between the transmit and receive antenna and the low noise amplifier (LNA) and the high-power amplifier (HPA). Diplexers are extensively used in satellite and wireless communication systems [1].

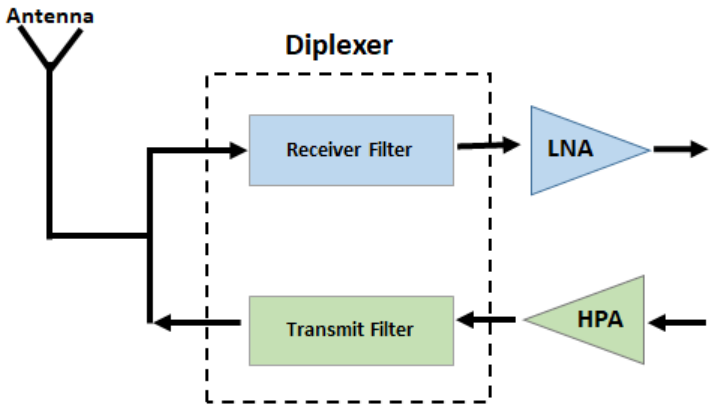

Figure 2-1 Conventional diplexer [1]

Through past decades different topologies have been used for multiplexers. The hybrid coupled multiplexer, formed by using a number of hybrid-coupled filter modules (HCFMs), is among the most used configurations [1]. A basic HCFM shown in Figure 2-2 consists of two identical bandpass filters, with two 90° (quadrature) hybrids. The structure has four ports. Based on the characteristics of the quadrature hybrid, the out-of-band signals entering from port 4, after reflection by the two channel filters, will be recombined in the hybrid to emerge from port 1. The in-band signals entering at port 3 will also emerge at port 1, combining with out-of-band signals of port 4. And finally, the remaining signal will be absorbed by the termination at port 2.

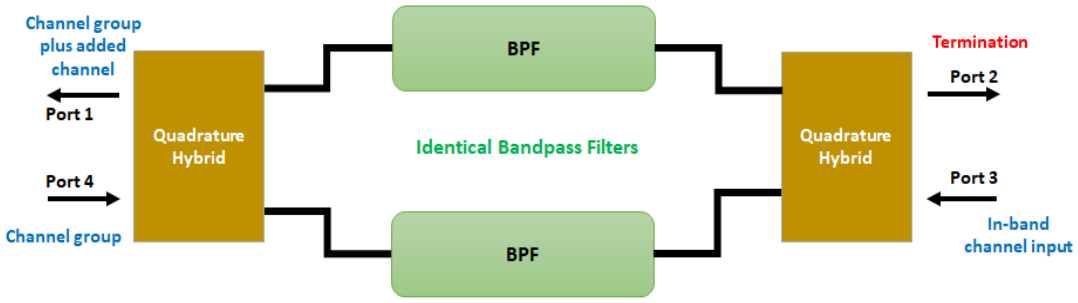

Figure 2-2 Hybrid-coupled filter module (HCFM) [1]

A multiplexer can be formed by connecting a number of HCFMs using transmission lines, as shown in Figure 2-3. A diplexer can also be implemented using HCFM, as will be demonstrated in Chapter 4 of the thesis.

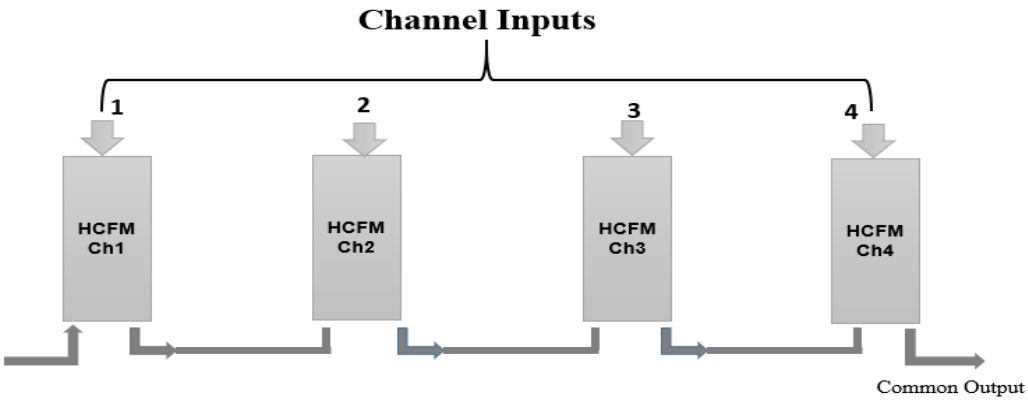

Figure 2-3 An HCFM-based multiplexer [1]

For high power applications, multiplexers are typically implemented using rectangular waveguides. Regardless of their many advantages, the conventional rectangular waveguides are difficult to integrate with planar structures, bulky in size and costly to fabricate. A new design of HCFM using rectangular waveguides with reduced size is presented in [2]. The 30% reduction in size comparing to conventional HCFM was achieved by introducing coupling between the two identical bandpass filters, and by eliminating a significant portion of the conventional quadrature hybrid.

Studies conducted in [3] and [4] present a different method of designing waveguide diplexer. These studies use the single and dual-band cavities, or a combination of both, to eliminate the requirement of junctions. Using lower number of cavities resulted in footprint reduction comparing to conventional designs.

A waveguide diplexer employing a new resonant three-port Y-junction is presented in [5]. Y-junction plays the role of a common dual-mode resonator for both channel filters, resulting in size reduction of the rectangular waveguide diplexer.

2.2 Substrate Integrated Waveguide

The rapid growth of technology and miniaturization of electronic devices in the telecommunication industry necessitate the use of more compact structures, such as substrate integrated circuits (SICs), replacing the bulky rectangular waveguide. The SIW technology for the past decade has been extensively investigated as a good alternative to conventional waveguides for many applications [6-8]. In addition to significant size reduction, SIW circuits can be easily integrated with planar circuits. At the same time, SIW offers lower loss than conventional planar circuits, such as microstrip circuits.

An SIW is similar to a dielectric filled rectangular waveguide, with embedded rows of metalized via holes as shown in Figure 2-4. The metalized via posts connect the two conductors on both sides of the substrate.

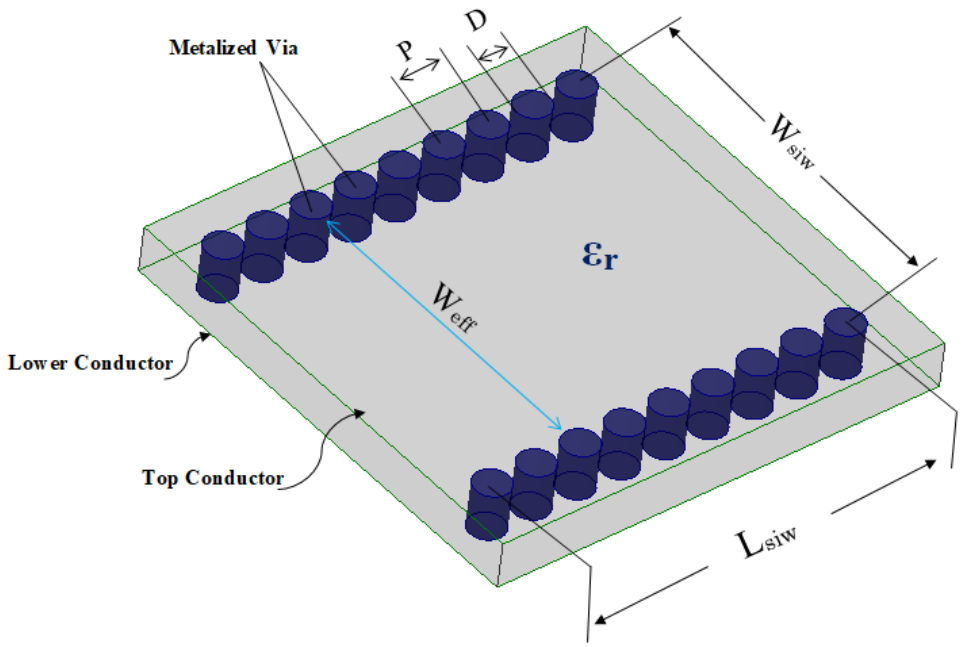

Figure 2-4 Geometry of substrate integrated waveguide (SIW)

A rectangular waveguide supports the transverse magnetic (TM), and transverse electric (TE) modes of propagations. However, in SIW structure the distance between the two adjacent vias creates discontinuity for the surface current, which results in vanishing of TM modes in SIW. The propagation modes in SIW structure are TEn0 modes and TE10 remains the dominant mode in SIW [9-12]. The operational frequency in SIW is determined by the width of SIW. Referring to Figure 2-4, an SIW structure is physically realizable if $P > D$, where P is the distance between two adjacent vias and D is the diameter of a via. To reduce the leakage loss to its minimum level, the distance P must satisfy the condition of $P \leq 2D$ [10]. The same study also suggests:

$$\frac{P}{\lambda_c} < 0.25 \tag{2.1}$$

where λ_c is the cut-off wavelength of the SIW. Respecting the above condition will eliminate the possibility of having a bandgap in the operational bandwidth.

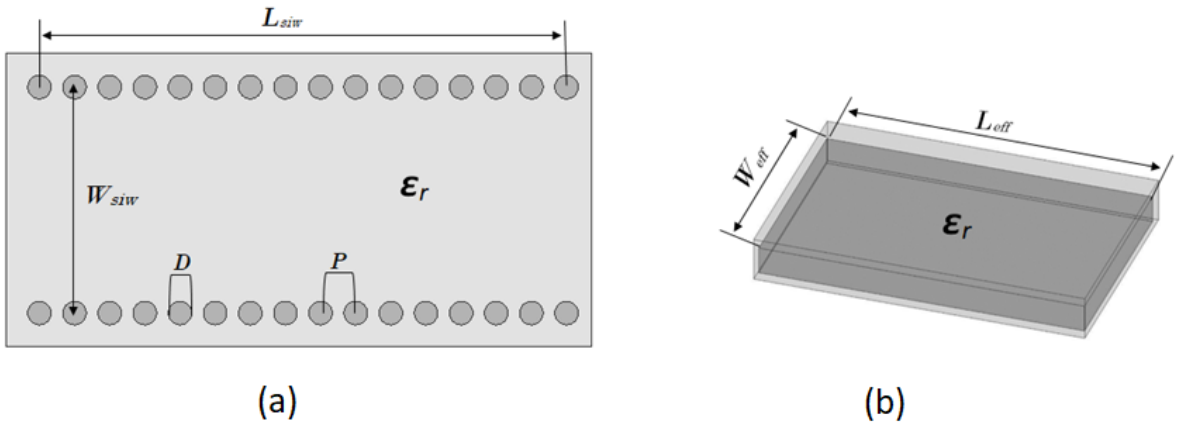

Figure 2-5 (a) SIW, and (b) its equivalent rectangular waveguide filled with the same dielectric [13]

An SIW can be represented using an equivalent rectangular waveguide, as shown in Figure 2.5, using the following equations [13-14].

$$W_{siw} - \left(\frac{D^2}{0.95*P}\right) = W_{eff} \quad (2.2)$$

$$L_{siw} - \left(\frac{D^2}{0.95*P}\right) = L_{eff} \quad (2.3)$$

where W_{eff} and L_{eff} are the width and length of equivalent rectangular waveguide filled with the same dielectric ε_r. The cut-off frequency of the dominant mode in SIW can be calculated using [15]:

$$f_c = \frac{c}{2*W_{eff}\sqrt{\varepsilon_r}} \quad (2.4)$$

A more accurate equation, as shown below, considers the effect of the ratio D/W_{siw}, where $P/D < 3$ and $D/W_{siw} < 0.2$ [16-18].

$$W_{eff} = W_{siw} - 1.08\frac{D^2}{P} + 0.1\frac{D^2}{W_{siw}} \quad (2.5)$$

The loss mechanism is important in the operation of an SIW structure, especially as the operational frequency grows higher [17]. There are three main sources of losses for SIW structure, namely dielectric loss, conductor loss, and radiation loss. Details are analyzed in [19-21]. The dielectric loss can be reduced simply by selection of substrate with better dielectric loss. The conductor loss in SIW is low comparing to other planar circuits, such as microstrip or stripline. Finally, as mentioned earlier, ensuring $P \leq 2D$ in the design of SIW will reduce the radiation loss.

SIW has been extensively used in all kinds of RF & microwave circuits, including filters, due to its relatively low insertion loss, or higher Q factor, comparing to other planar circuits, compact size, low fabrication cost, and ease of integration with other planar

circuits. A complete study on the basic design aspects and practical features of the SIW filters has been conducted in [19].

SIW has also been used for diplexer design. A multilayer balanced SIW-based diplexer is presented in [22] using single and dual mode resonators. The study achieves the size reduction of the diplexer by using vertically stacked SIW cavities. *K*-band SIW technology-based diplexers are presented in [23-24]. The diplexer in [23] uses a dual mode cavity junction as a transition, and the junction also supplies each channel filter with one pole. A *C*-band diplexer presented in [25] uses hybrid SIW and coplanar waveguide to achieve high selectivity, isolation, and size compactness.

2.3 Tunable Microwave Filters and Multiplexers

Tunable microwave circuits, including tunable filters, have attracted a lot of attentions as they add agility to a communication system. Different tuning techniques have been developed for tuning SIW filters. Studies conducted in [26-29] present mechanical tuning methods of SIW filters. Tuning of SIW structure is also important to compensate the mechanical tolerance and dielectric permittivity tolerance of SIW substrate [27].

Magnetic tuning using single and double ferrite slab loaded SIW cavity is presented in [30]. Simultaneous electric and magnetic tuning is realized using varactor diode and ferrite slab to tune center frequency and bandwidth of the filter in [31]. Via-posts and RF MEMS switches are used to tune SIW filters in [32]. Study conducted in [33] uses combination of metallic via posts with pin diode switching elements for tuning SIW filter, while [34] achieves tunable SIW filter by using only the pin diode without requiring the metallic post. Work presented in [35-36] uses surface mount varactor diodes for tuning the center

frequency of SIW resonators. The studies in [37-39] employ varactor diodes as the tuning element for tuning center frequency and bandwidth of the SIW filter.

Tuning multiplexer is more challenging comparing to tuning a single filter, due to the interaction among channels. There are limited reports on techniques for tuning multiplexers or diplexers.

An electronically tunable microstrip diplexer consisting of a pairs of tunable dual-mode bandpass filters is presented in [40], and varactor diodes were used to achieve the tunability of the diplexer.

In a tunable cavity diplexer proposed in [41], tuning screws are used to control the resonant frequency of the diplexer. A tunable diplexer with high selectivity and isolation, consisting of two different tunable filters, is presented in [42]. The tunability of each channel filter and of the diplexer was achieved by employing varactor diodes. The authors in [43] use a tunable diplexer for designing a wide frequency range bandpass filter.

In [44], the authors take a different approach. The interference between two channels of a diplexer is studied. An additional path between the two channels is introduced, which generates a cancellation effect and helps to avoid performance deterioration during tuning. A combline tunable diplexer using tuning screws is used to demonstrate the design principle. The study in [45] investigates a synchronously tuned trimode resonator for designing a frequency-adaptive bandpass diplexer. It demonstrates frequency duplexing of constant absolute bandwidth with two identical passbands. Varactor diodes are used to achieve required tuning range.

For diplexer implemented using SIW technology, the study conducted in [46] presents a tunable SIW diplexer employing stepped impedance resonators, varactor and electro-static MEMS on their different SIW tunable diplexers. The work in [47] presents a multilayer SIW tunable diplexer, where both channels of the diplexer are tuned independently from each other by employing varactor diodes.

Chapter 3

Hybrid-Coupled Filter Module (HCFM) using Substrate Integrated Waveguide (SIW)

3.1 Design process of HCFM using SIW technology

A conventional hybrid-coupled filter module (HCFM) shown in Figure 2-2 consists of two identical bandpass filters (BPFs) and two 90° (quadrature) hybrids. An improved HCFM using rectangular waveguide technology with size reduction was designed in [2] as shown in Figure 3-1. The improved module in [2], referred as the improved HCFM here, achieved 30% size reduction comparing to conventional design using rectangular waveguide. The important reduction of footprint was achieved by introducing the inter-resonator coupling between the two filters in HCFM, and consequently removing part of the conventional 90° hybrids.

In Figure 3-1(a), the transmission line L_1 is the length of the waveguide from the center of T-junction to the input coupling of the filter. The waveguide L_2 is the distance between the two T-junctions or the distance form port 1 to port 4 in the improved HCFM. The initial values of both L_1 and L_2 is $\lambda/4$, where λ is the guided wavelength of the waveguide [2]. The impedance of L_1 and L_2 are Z_1 and Z_0, respectively. $K'_{01} = \sqrt{2}Z_1K_{01}$ and $K_{02} = {K_{01}}^2$, where Z_0 is normalized to be 1, K_{01} is the filter input coupling in a conventional standalone filter, K'_{01} is the filter input coupling in the improved HCFM, and K_{02} is the inter-resonator coupling between two filters.

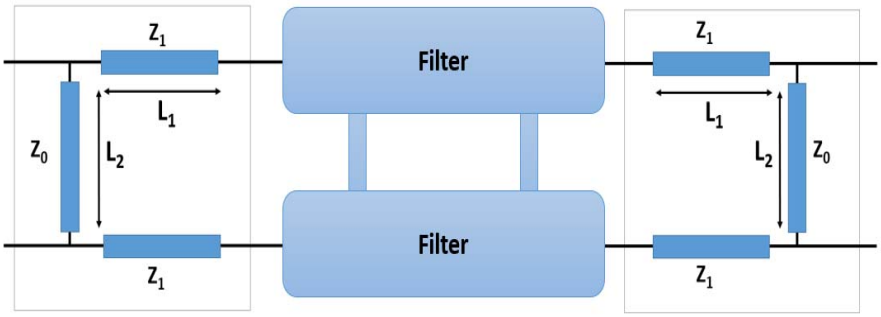

(a)

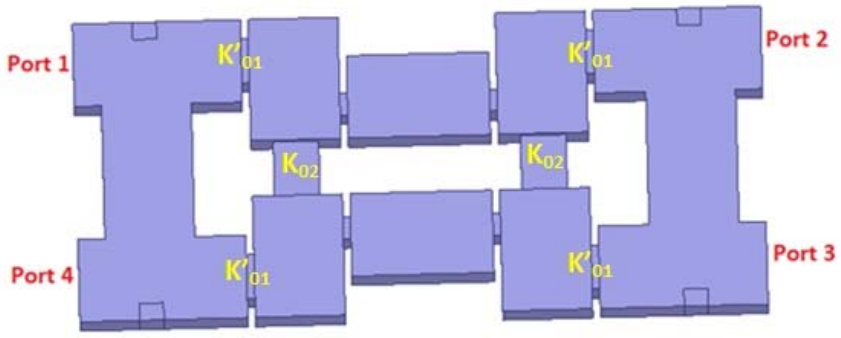

(b)

Figure 3-1 Improved Hybrid-Coupled Filter Module (HCFM) [2]: (a) block diagram, and (b) waveguide implementation

This chapter presents an improved HCFM using substrate integrated waveguide (SIW) technology, which results in even further reduction in size. In addition, unlike rigid rectangular waveguide, the SIW allows flexibility in the layout and waveguide design variables. This enables further reduction in the footprint. As shown in the topology in Figure 3-2, the physical distance between two filters can be reduced to almost zero in the new design. Therefore, the SIW HCFM achieves a total footprint reduction of 60% comparing to the improved HCFM shown in Figure 3-1 [2].

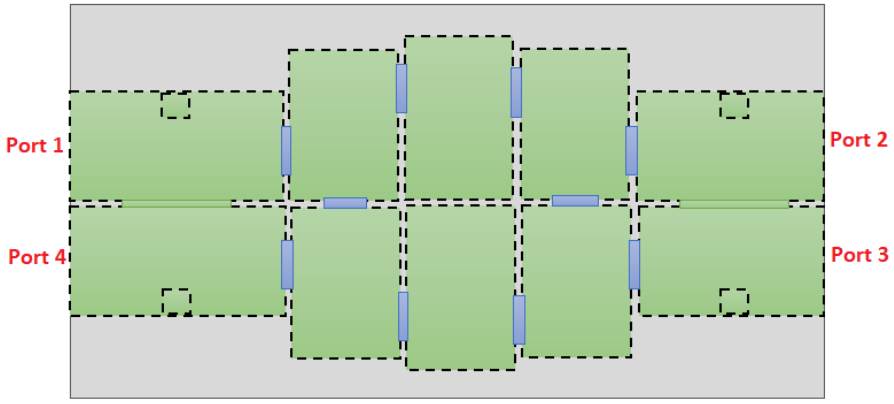

Figure 3-2 Topology used for the improved HCFM using SIW

As discussed in chapter 2, an SIW is essentially a dielectric filed waveguide. Hence the design process of improved HCFM using SIW is similar to the design process presented in [2]. The substrate RT/duroid®6002 with a thickness of 0.02 in and relative permittivity ε_r = 2.9 is used to design the improved HCFM using SIW technology. Referring to Figure 2-4, W_{siw} = 0.452 in, L_{siw} = 0.7 in, dimeter of the metallic via of 0.026 in, and the distance between two adjacent vias P is 0.042 in.

The equivalent circuit model of the HCFM in ADS is shown in Figure 3-3. Figure 3-4 presents the S-parameters of the equivalent circuit model. The center frequency of the HCFM is 12.44 GHz with a bandwidth of 200 MHz, the $|S_{11}|$ and $|S_{12}|$ for the entire frequency range of interest are below -15 dB. The $|S_{13}|$ and $|S_{14}|$ of the HCFM have identical functionality as the transmission and reflection coefficients of a standalone bandpass filter, respectively.

The design process of the improved HCFM using SIW technology involves the following steps shown in Figure 3-5.

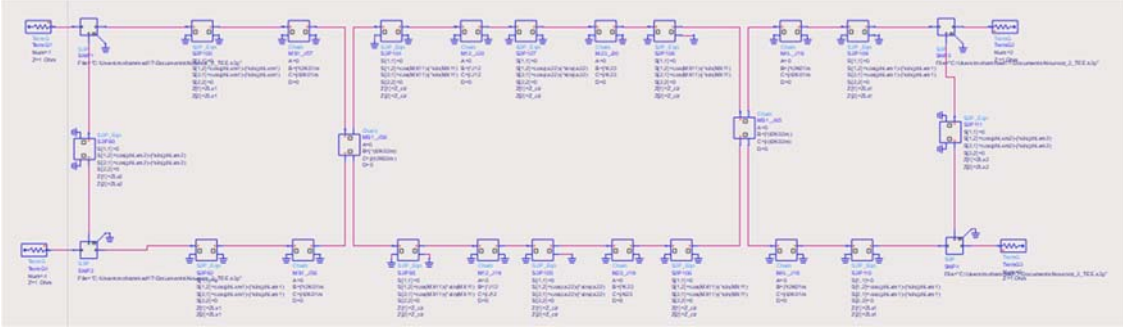

Figure 3-3 Equivalent circuit model of the HCFM in ADS

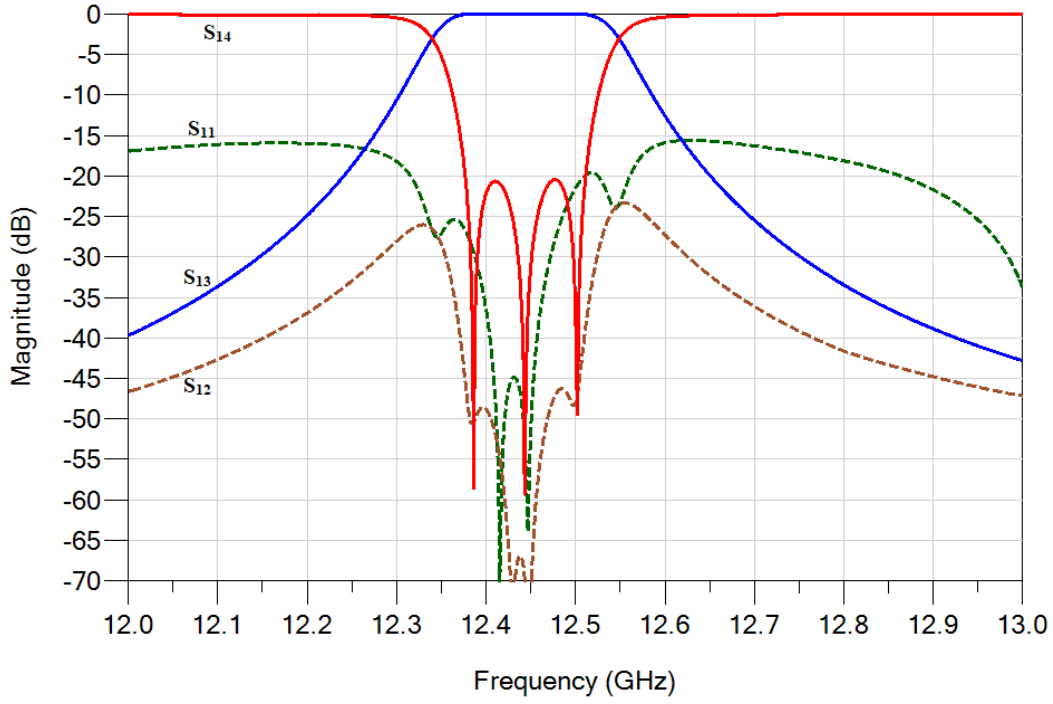

Figure 3-4 S-parameters generated in ADS of the 3poles filter HCFM at 12.44 GHz

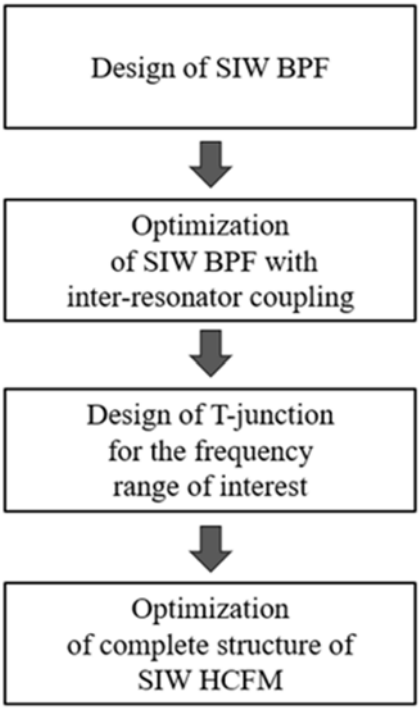

Figure 3-5 Flow chart of designing the improved HCFM using SIW

3.1.1 Design of a three poles SIW bandpass filter

The goal of this step is to design a standalone SIW bandpass filter, operating at 12.44 GHz with 20 dB return loss in the pass band, as a starting point for the HCFM.

Single cavity is the building block of the SIW cavity-based filter. The design process starts after converting a single rectangular waveguide cavity to its equivalent substrate integrated waveguide cavity (Figure 2-5) using equations provided in chapter 2. The eigenmode in HFSS is used to calculation the SIW cavity size and coupling irises dimensions, which are subsequently used as initial dimensions for the filter model in HFSS.

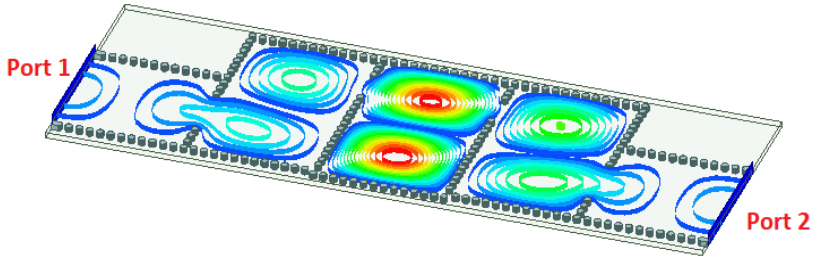

Figure 3-6 SIW 3Poles BPF in HFSS

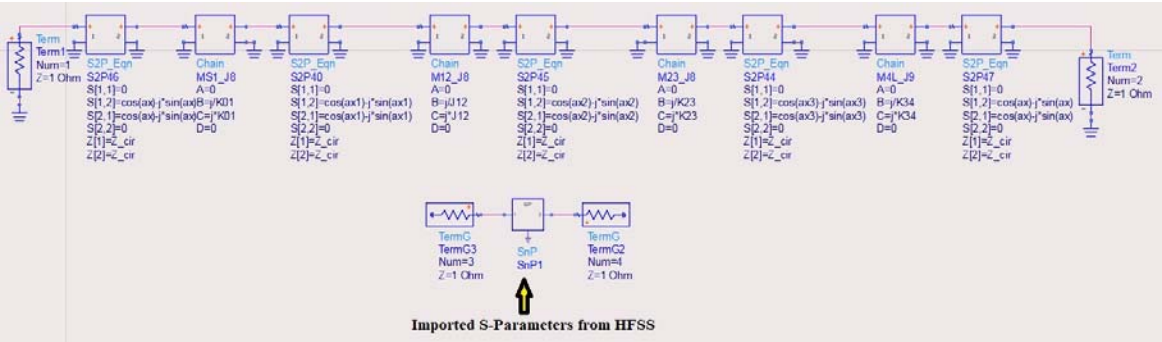

Figure 3-7 Equivalent circuit model of 3 poles BPF in ADS

Figure 3-6 shows a three poles SIW bandpass filter that is built in HFSS using initial dimensions. The mode of operation for each cavity is TE102 mode. Cavities are coupled side by side, instead of end coupled, which helps to reduce the footprint of the overall design. The two identical filters in the improved HCFM using SIW as shown in Figure 3-2 will be using similar topology in Figure 3-6.

A circuit model in ADS as shown in Figure 3-7 is used to compare the imported S-parameters from HFSS with the S-parameters generated from the equivalent circuit model in ADS. This comparison will indicate how far the model in HFSS is from the target model in ADS. The tuning process enables us to visualize the effect of changing the design parameters by comparing the results with the imported S-parameters from HFSS. This comparison will help us to decide how to change certain parameters, such as length of the

cavity or coupling irises in HFSS model, to control the operational frequency or bandwidth of the filter correspondingly. This tuning process continues until the extracted coupling values based on responses from HFSS agree to the ideal coupling values in ADS.

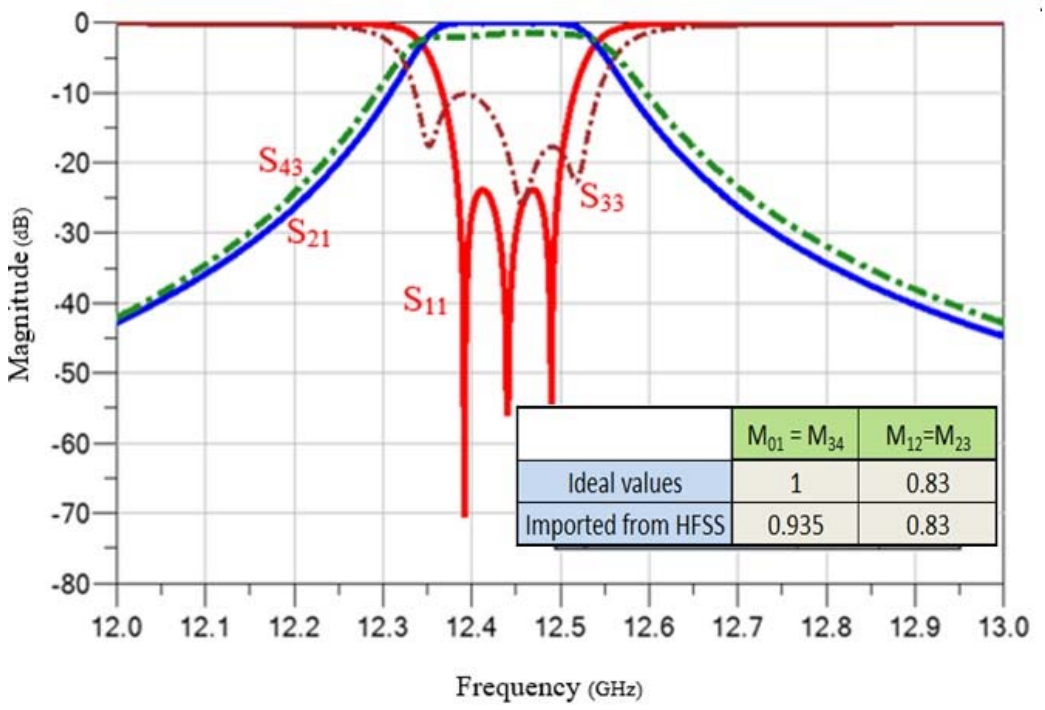

Figure 3-8 Comparison of S-parameters of HFSS with ideal circuit model results in ADS (solid lines: circuit model results, dashed lines: EM simulation results)

The imported S-parameters from HFSS ($|S_{33}|$ and $|S_{43}|$) against the ideal response in ADS ($|S_{21}|$ and $|S_{11}|$), as shown in Figure 3-8, indicate the 3poles BPF model in HFSS has the same operational frequency of 12.44 GHz, but different coupling values. Corresponding dimensions in HFSS are changed and extracted coupling values in ADS are compared with ideal values again.

Figure 3-9 and Figure 3-10 show a good agreement of the S-parameters for both models achieved after few iterations. The requirements of 12.44 GHz center frequency, with a 20 dB return loss in operational bandwidth are satisfied.

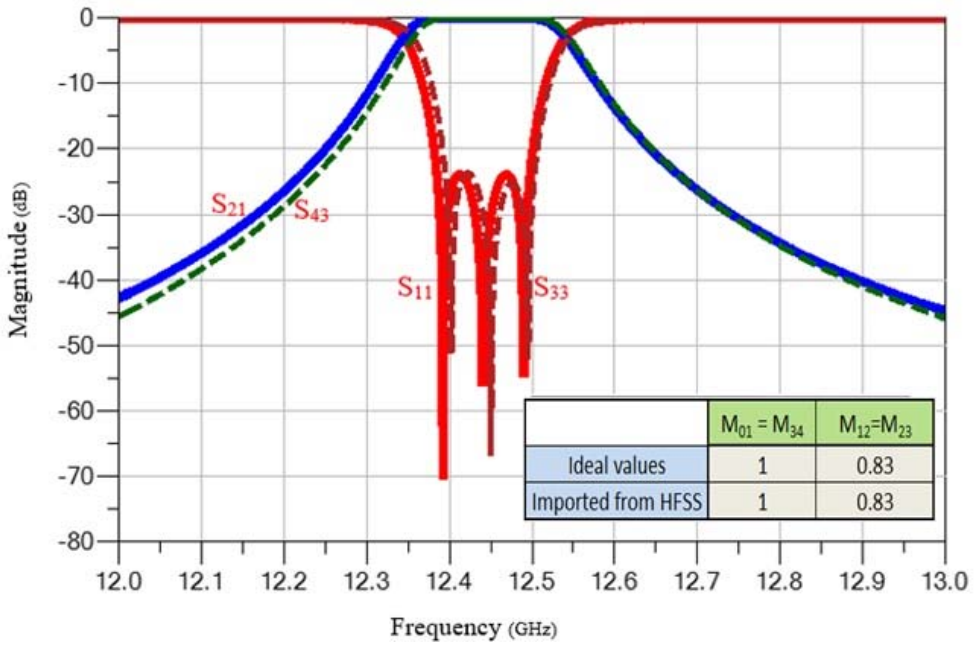

Figure 3-9 Comparison of optimized S-parameters of HFSS with circuit model results in ADS in step 1

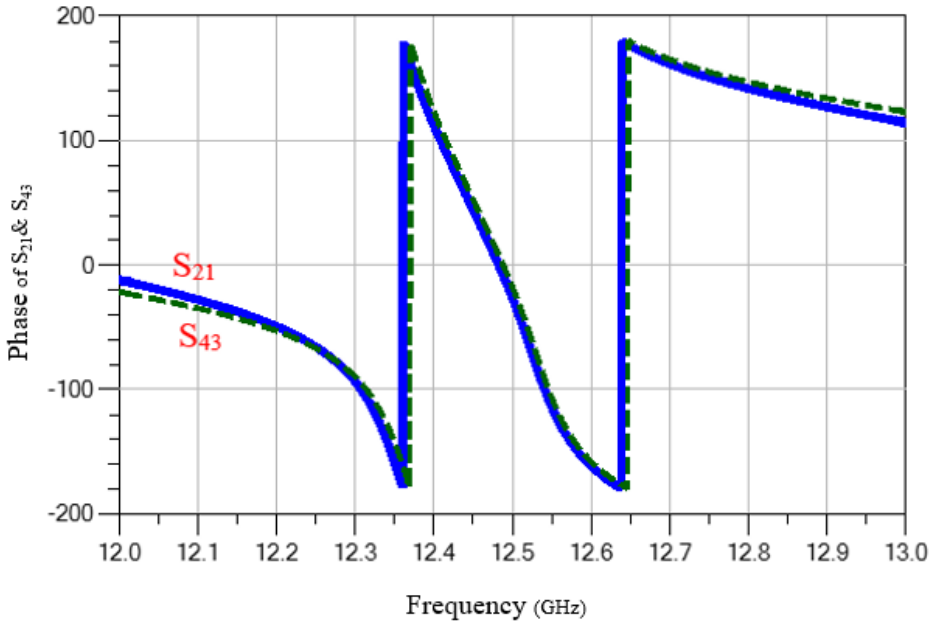

Figure 3-10 Comparison of phase of S-parameters using HFSS and ADS in step 1

3.1.2 Optimization of the three-pole BPF including inter-resonator coupling

The improved HCFM using rectangular waveguide technology presented in [2] suggests an inter-resonator coupling between the two identical bandpass filters of the HCFM as shown in Figure 3-1. The coupling was added in the first and last cavity of the bandpass filters as shown in Figure 3-11. In addition, comparing to the previous step, the input and output coupling (M_{01} and M_{34}) are increased. The coupling values are listed in Figure 3-12. The target of this step is to take these requirements into account by optimizing the structure in Figure 3-11.

Optimization procedure is similar to the previous step. Figure 3-12 and Figure 3-13 indicate good agreement between the S-parameters of the model in HFSS and circuit model in ADS for the three poles bandpass filter operating at 12.44 GHz.

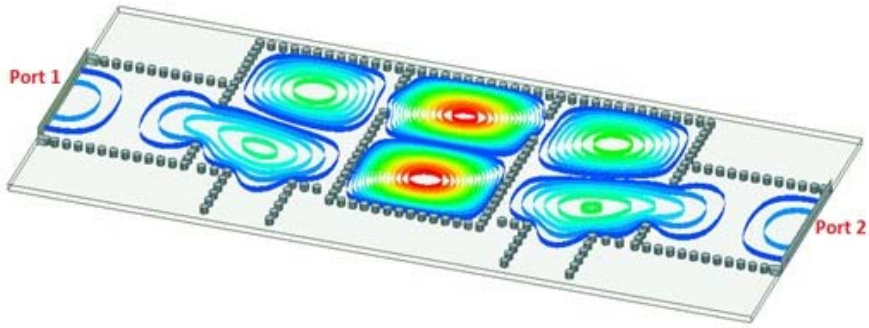

Figure 3-11 3Poles SIW BPF with openings in the first and last cavity

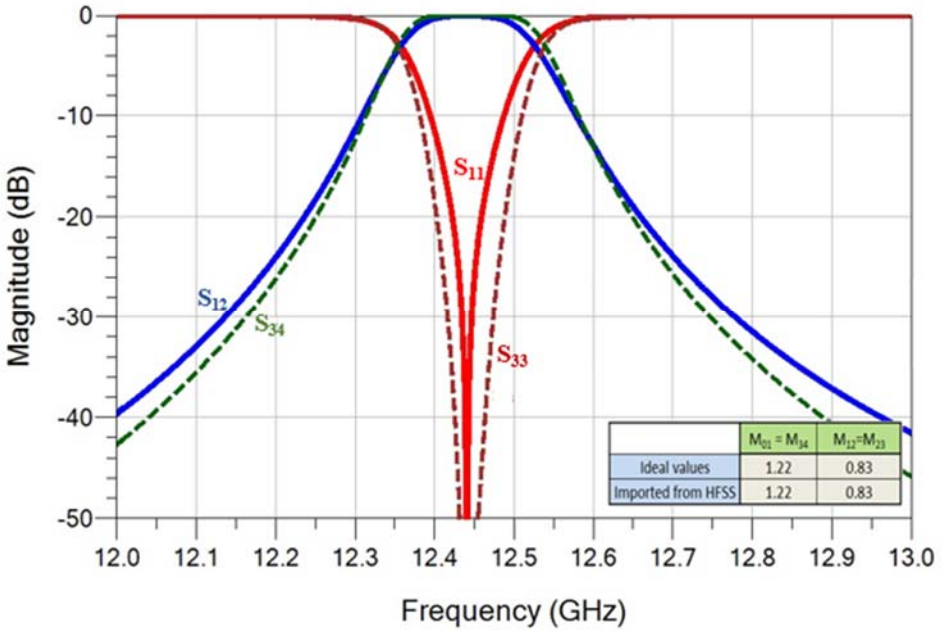

Figure 3-12 S-parameters of BPF with opening in first and last cavities (solid lines: circuit model results, dashed lines: EM simulation results)

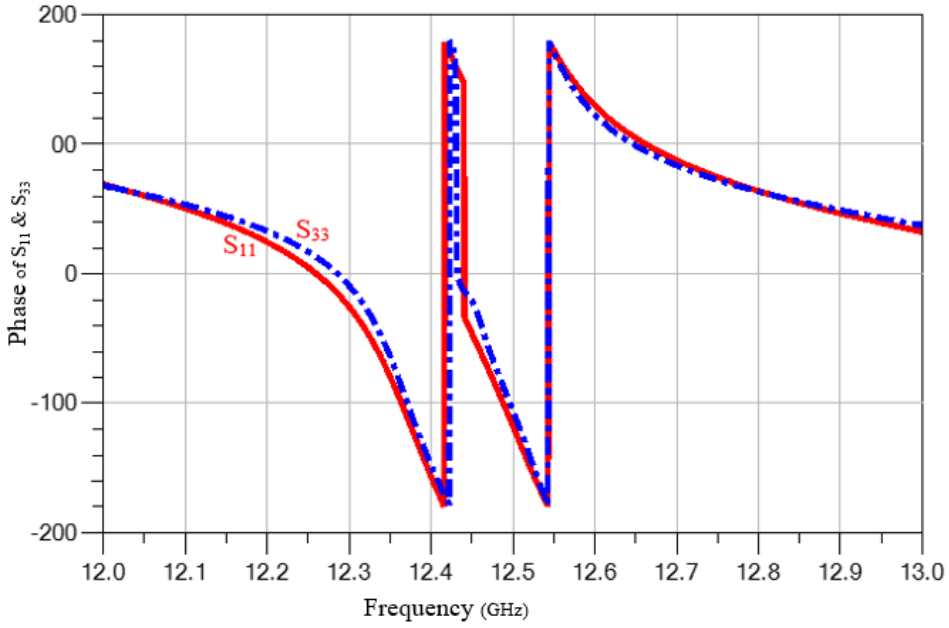

Figure 3-13 Phase of S_{11} and S_{33} of 3-pole BPF with inter-resonator coupling

3.1.3 Design of T-junction power divider

Directional couplers and power dividers are passive components that are used to combine or split the power. The T-junctions as three port dividers are the simplest forms of power dividers. There are usually two simple topologies that are used for the design of the T-junction, a Y-shaped topology where each channel is 120º apart, and a T-shaped junction with 90º between each channel. For the purpose of this design a T-shaped topology as shown in Figure 3-14 is used.

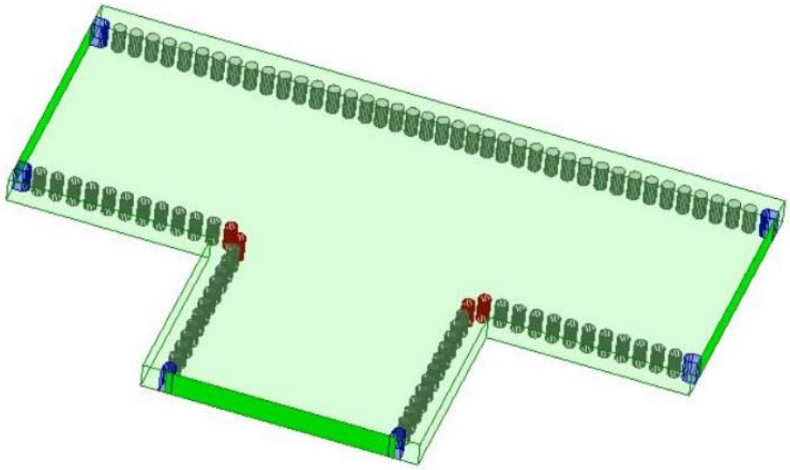

Figure 3-14 T-junction power divider

An ideal 3 dB coupler splits the power entered from one of the ports, equally into other two ports [2]. In SIW T-junction the entered power from one of the ports will not be directed equally into other two ports, and requires modifications. The T-junction requires a post, as shown in Figure 3-15, to be able to split the power equally between ports 2 and 3.

The S-parameters results for the modified T-junction are shown in Figure 3-16, where $|S_{21}|$ and $|S_{31}|$ are similar in the entire frequency range of interest for the HCFM.

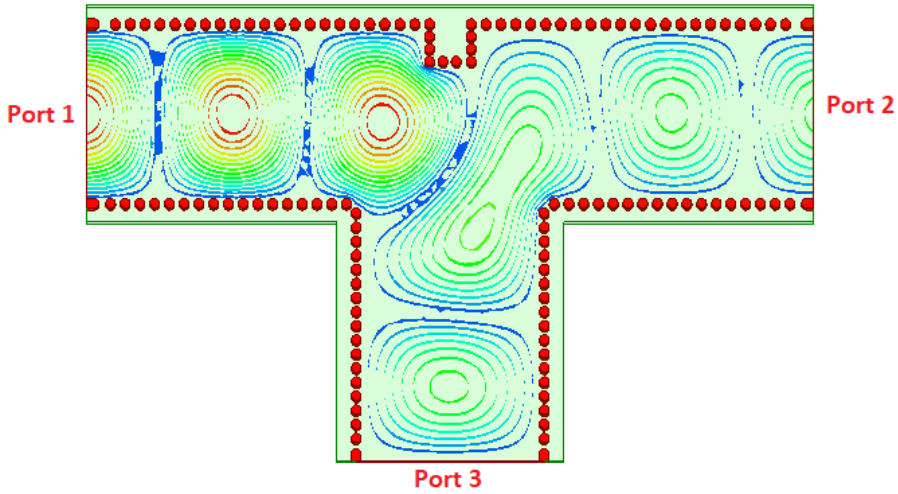

Figure 3-15 Modified T-Junction power divider

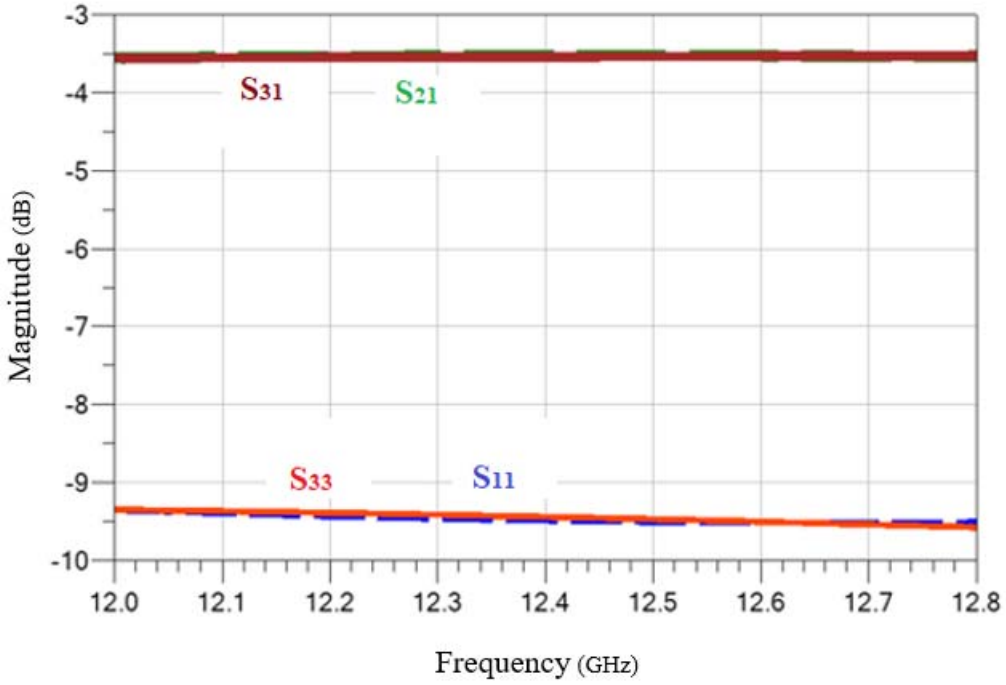

Figure 3-16 S-Parameters of the modified T-junction power divider

3.1.4 Complete design of the improved HCFM using SIW

The final step in the design of the improved HCFM using SIW is to optimize the final structure shown in Figure 3-17. An improved HCFM is comprised of two identical

bandpass filters and waveguide T-junctions (reduced quadrature hybrids) as shown in Figure 3-17. The bandpass filters are connected using inter-resonator coupling at the first and last cavities, respectively. As mentioned earlier, the orientation of cavities helps to reduce the size of the HCFM.

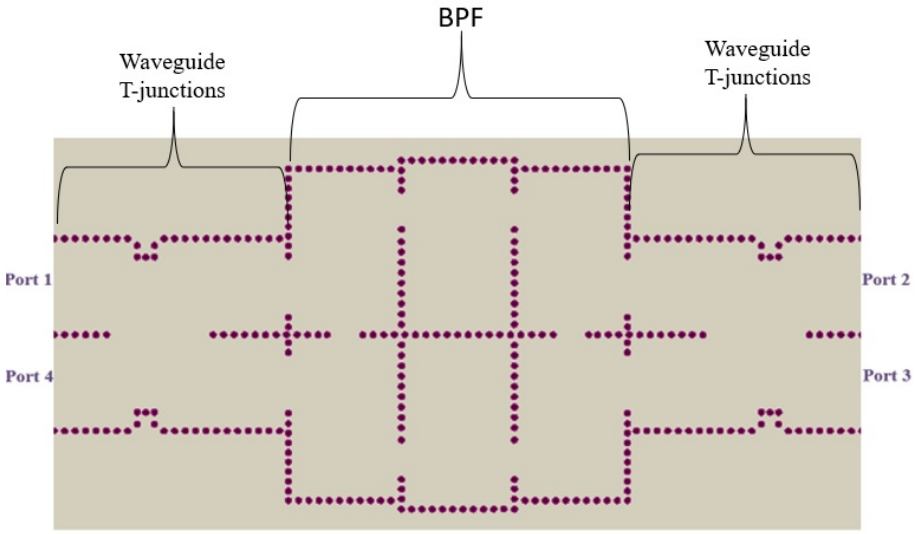

Figure 3-17 Low-profile improved HCFM using SIW

Referring to Figure 3-17, for the design presented in this thesis for the improved HCFM using SIW, the distance between the two filters and also the waveguide connecting the two T-junctions in the reduced 90º quadrature hybrids are eliminated. This elimination resulted in even more compact size of the improved HCFM using SIW technology.

Despite the successful completion of the previous steps, the complete structure in Figure 3-17 still requires the final optimization to meet the requirements. In addition to the previous elements of optimization such as coupling irises, length of cavities, and inter-resonator coupling between the bandpass filters, a number of new design parameters are optimized.

Figure 3-18 shows these new parameters for optimizing the improved SIW HCFM, including the distance from the center of the T-Junction to the first coupling iris of the filter, L, D_1, and D_2.

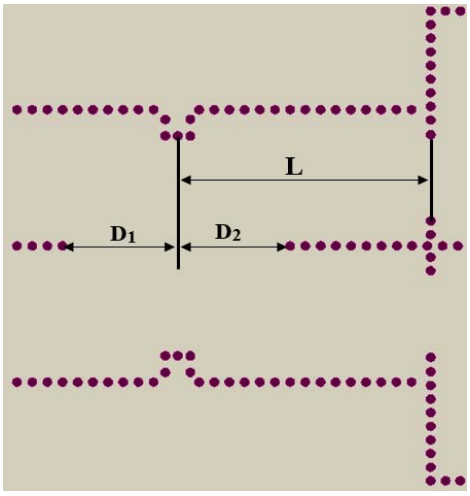

Figure 3-18 Quadrature hybrid using SIW

The S-parameter results of EM simulation in HFSS for the improved HCFM using SIW are shown in Figure 3-19. The results indicate that the $|S_{13}|$ and $|S_{14}|$ of HCFM behave similarly to the transmission and reflection coefficients of a standalone bandpass filter, respectively. Furthermore, the $|S_{11}|$ and $|S_{21}|$ of the HCFM are below -12dB for the entire frequency range (12 to 13 GHz). These results are in good agreement with the results of the circuit model in ADS shown in Figure 3-4. This completes the design of the improved HCFM using SIW.

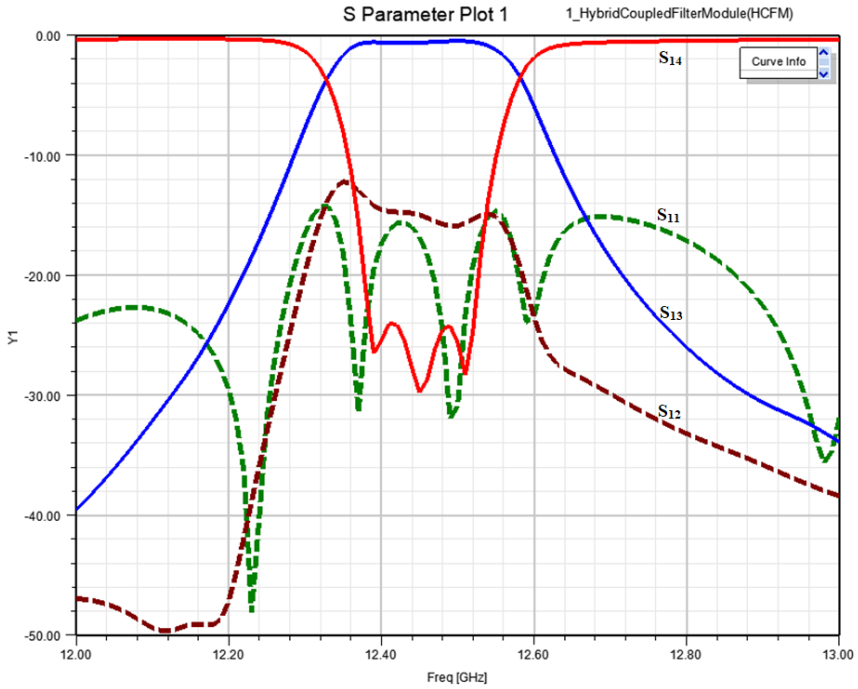

Figure 3-19 S-parameters of the improved SIW HCFM operating at 12.44 GHz

3.2 Microstrip to SIW Transition

For the purpose of measurement, the HCFM using SIW still requires the design of a transition to SIW so that it can be connected to test equipment. Different transitions for SIW structure have been discussed in [48 – 50]. Figure 3-20 shows the microstrip to SIW transition taper, one of the most used transitions in single layer circuits. The functionality of the taper section is to transform the quasi-TEM mode of microstrip line into TE10 mode in SIW [48].

Referring to Figure 3-20, the design variables are W_{Taper} and L_{Taper}, which can be obtained through optimization using HFSS [51]. The goal is to keep $|S_{11}|$ as low as possible, i.e. good impedance matching, for the entire frequency range of interest. For this design, the optimized dimensions are L_{Taper} = 0.185 in and W_{Taper} = 0.137 in, which connects a 50 Ω

microstrip line to the SIW. As shown in Figure 3-21, $|S_{11}|$ of the designed back-to-back transition is lower than -25 dB for the entire frequency range (12 to 13 GHz).

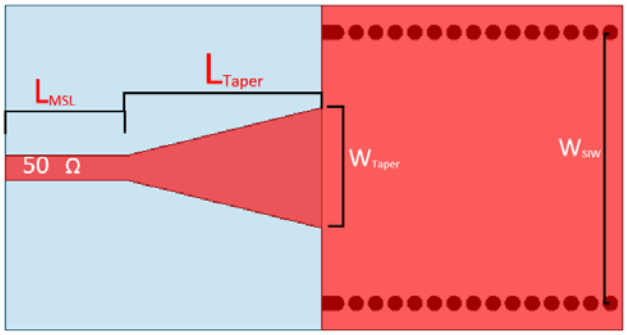

Figure 3-20 Microstrip to SIW transition taper

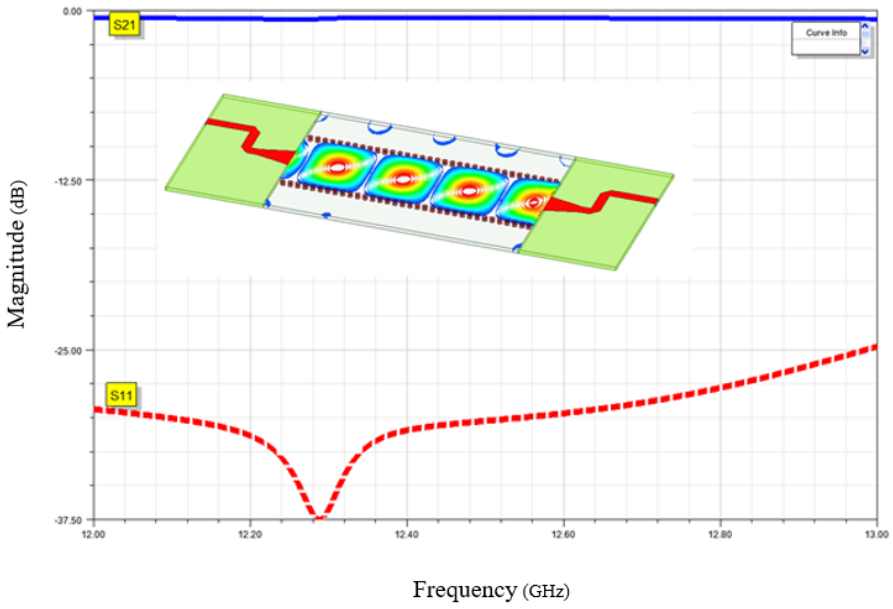

Figure 3-21 S-parameters of the microstrip transition taper to SIW

Figure 3-22 presents the improved HCFM using SIW technology with microstrip transitions. This design presented in this thesis meets the requirements, and also successfully achieves 60% size reduction comparing to the improved HCFM presented in [2].

The S-parameters are shown in Figure 3-23. The full EM simulations results in Figure 3-23(b) are in good agreement with the results of the circuit model in Figure 3-23(a). $|S_{11}|$ and $|S_{21}|$ are lower than -12 dB for the entire frequency range.

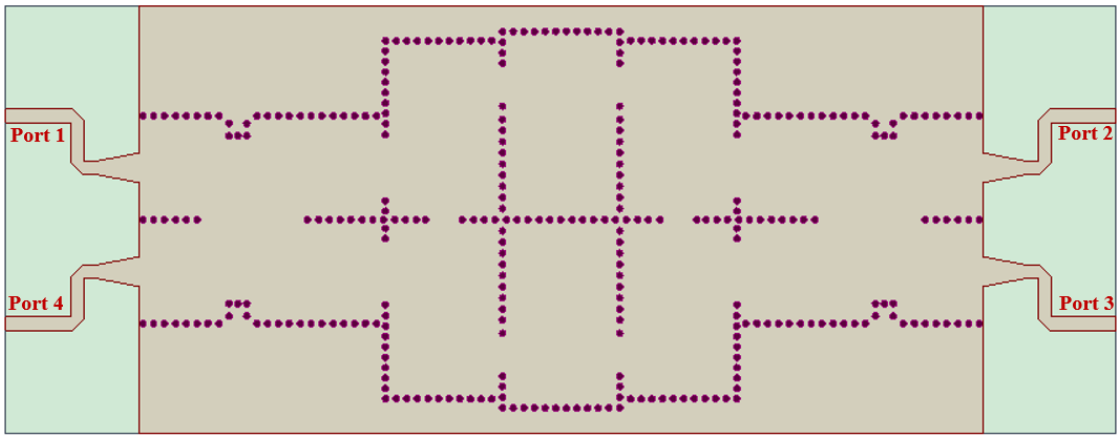

Figure 3-22 Compact SIW HCFM with microstrip transitions

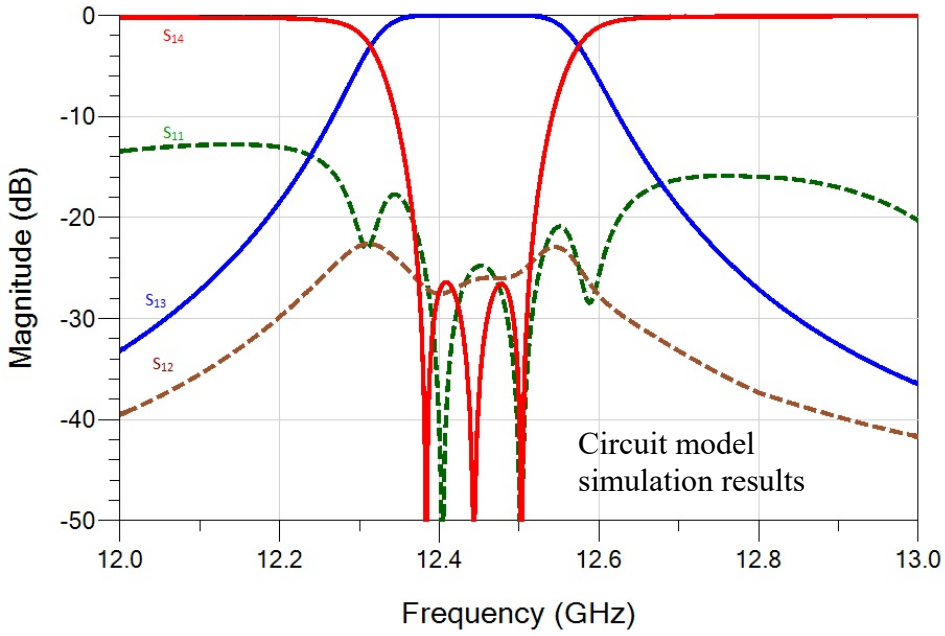

(a)

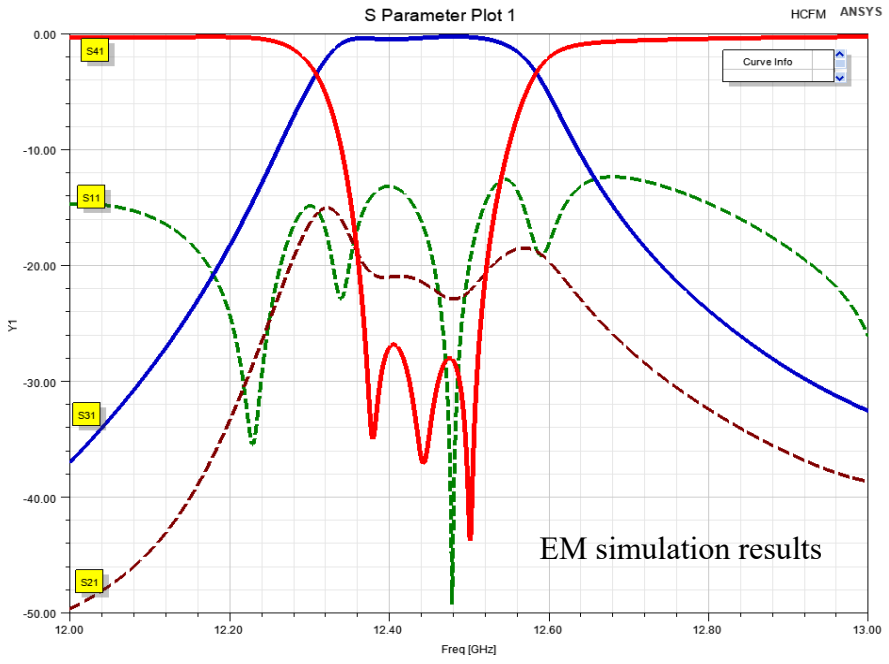

(b)

Figure 3-23 S-Parameters of the SIW HCFM with microstrip transition

3.3 Electronic tuning of the HCFM

With high demand of today's communication network for more compact in size and multifunctional devices, tunable multiplexers will be even more beneficial for the communication system. In this section, the feasibility of electronically tuning the HCFM is investigated employing varactor diodes as the tuning elements on the SIW cavity resonator and SIW HCFM. Furthermore, the effect of two tuning elements to achieve wider range of tunability is also discussed.

3.3.1 Electronic tuning of the single cavity resonator

For electronic tuning of an SIW cavity, a varactor diode can be used as the tuning element [35]. For the purpose of simulation of the tuning element in HFSS, as shown in Figure 3-24, a circular slot and metallic patch are created on the top conductor of the cavity. In order to achieve the best performance from the tuning device, strong interaction between the tuning element and the existing field inside the cavity is needed. This interaction depends on the distance from the where the maximum electric field is to the center of the slot, D_x, and also depends on the width of the slot, W_t. Referring to Figure 3-24, L_{SIW} = 0.806 in, W_{SIW} = 0.41 in, D_x = 0.03 in, and W_t = 0.024 in. A surface mount varactor diode (MAVR-011020-1411) is considered as the tuning element. According to the performance curve of the varactor diode, the capacitance of the diode varies from 0.035 pF to 0.15 pF as the reverse bias voltage decreases from 20 V to 1 V [52].

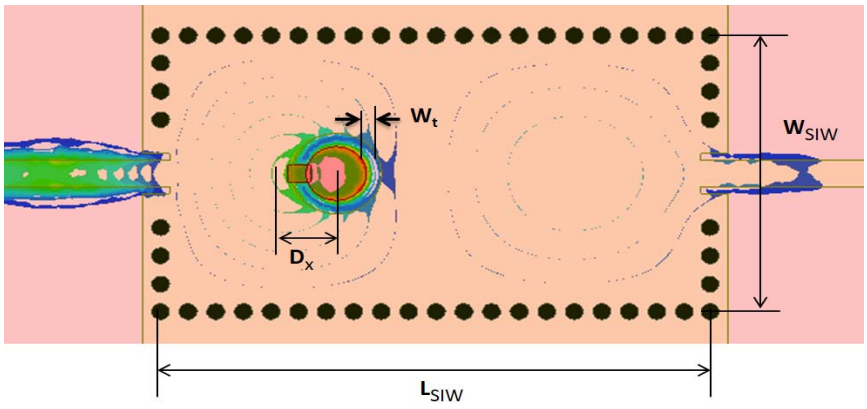

Figure 3-24 SIW cavity loaded with one varactor diode

For the purpose of simulation in HFSS, instead of using a varactor, the capacitance value is swept from 0.035 pF to 0.15 pF. The $|S_{11}|$ results of a single cavity resonator are shown in Figure 3-25. The center frequency of the SIW cavity resonator changes from 12060 MHz to 12520 MHz as the capacitance changes. Therefore, the varactor can provide a tuning range of 460 MHz.

Furthermore, two varactor diodes are employed on the same cavity to investigate the effect of two varactor diodes on the tuning range. The parameters in Figure 3-26 are L_{SIW}=0.806 in, W_{SIW}=0.41 in, D_x=0.03 in, and W_t=0.024 in.

The S-parameters of the SIW cavity resonator with two varactor diodes are shown in Figure 3-27. The capacitance is swept from 0.035 pF to 0.15 pF, which results in sweeping the center frequency of the SIW cavity from 11890 MHz to 12500 MHz. Therefore, the tuning range is increased to 610 MHz using two varactor diodes.

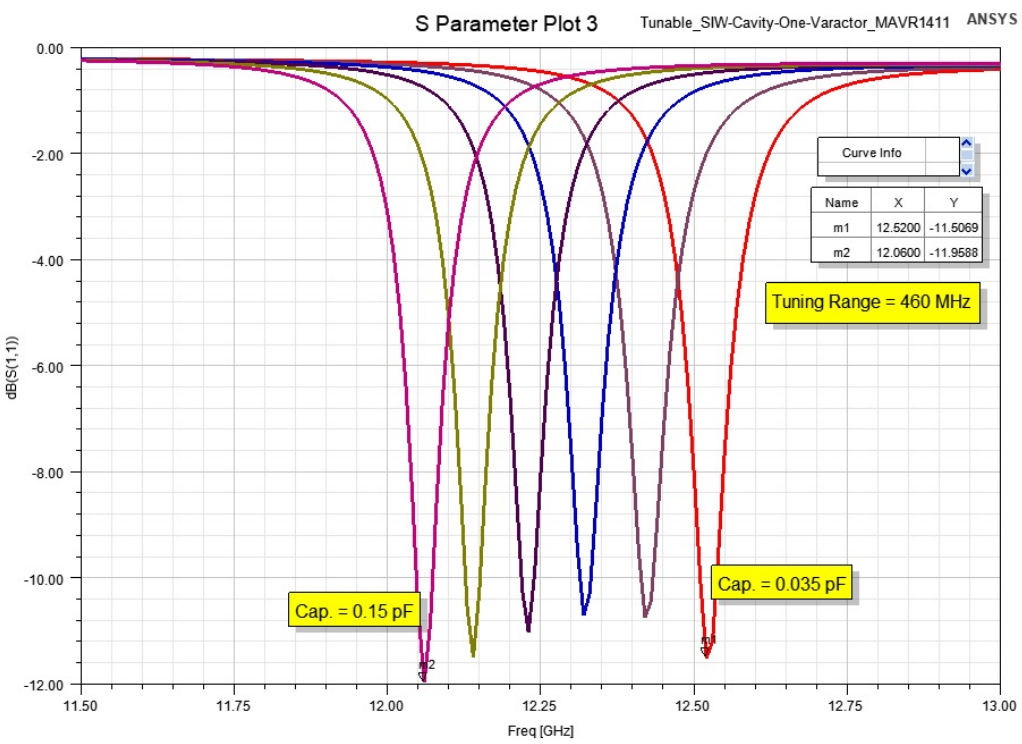

Figure 3-25 S-parameter of tunable SIW cavity using one varactor diode

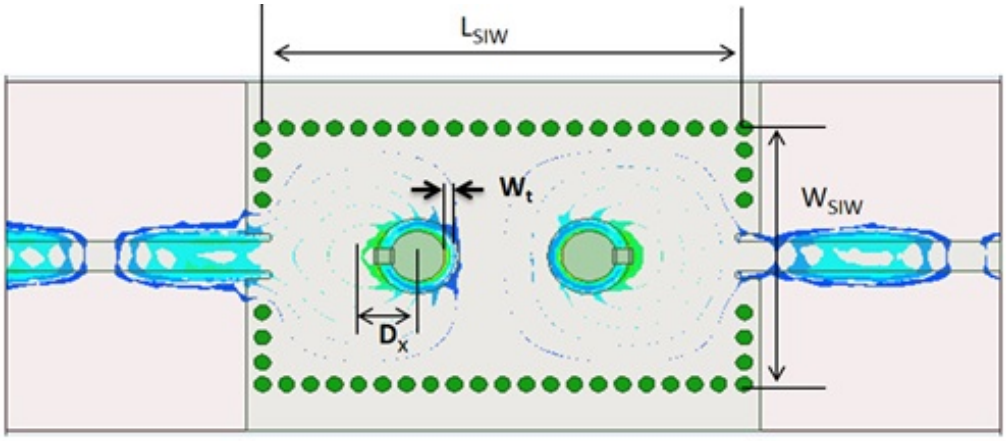

Figure 3-26 SIW cavity resonator loaded with two varactor diodes

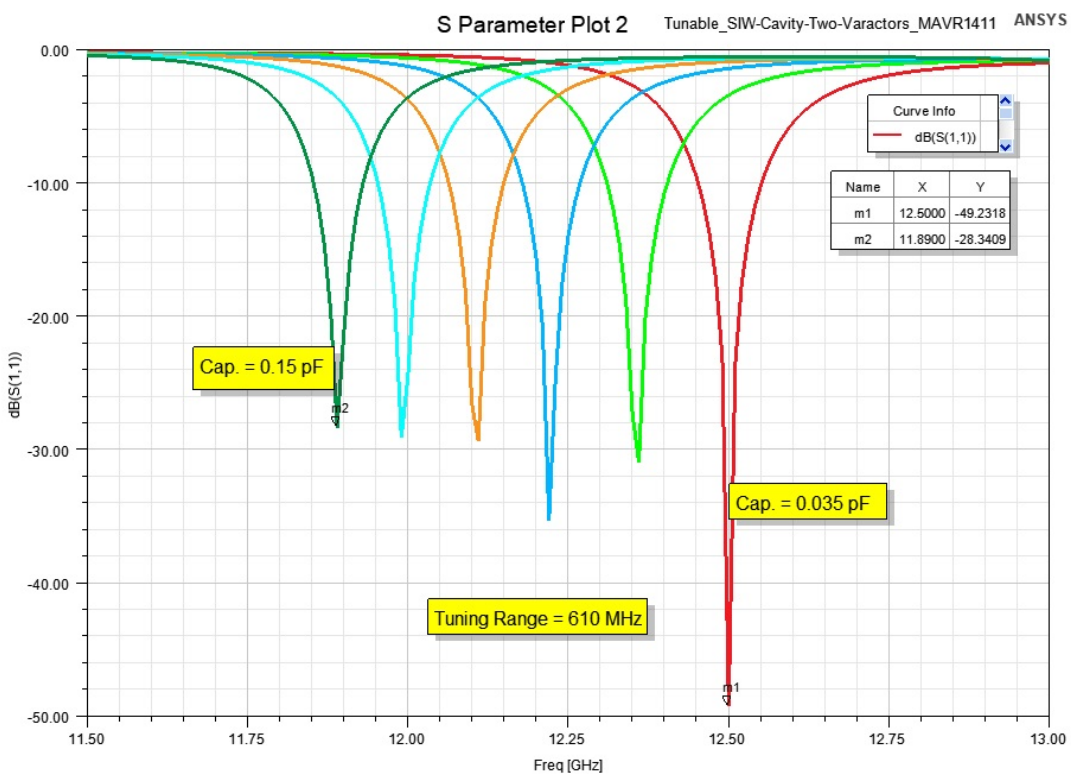

Figure 3-27 S-parameters of SIW cavity resonator using two varactor diodes

3.3.2 Electronic tuning of the improved HCFM

In this section, the SIW HCFM is simulated in HFSS for electronic tunability investigation. The same surface mount varactor diode, MAVR-011020-1411, is employed.

Six tuning elements are used as shown in Figure 3-28. The capacitance of the varactor diode varies from 0.035 pF to 0.15 pF as the reverse bias voltage decreases from 20 V to 1 V [52]. S-parameters of the SIW HCFM is shown in Figure 3-29. The operational frequency of the HCFM shows a tuning range of 231 MHz, while the return loss $|S_{14}|$ is below -18 dB for the entire range of tuning. In addition, it is possible to improve the tuning range by adding one more varactor diode in each cavity and tune the SIW HCFM using total of twelve varactor diodes.

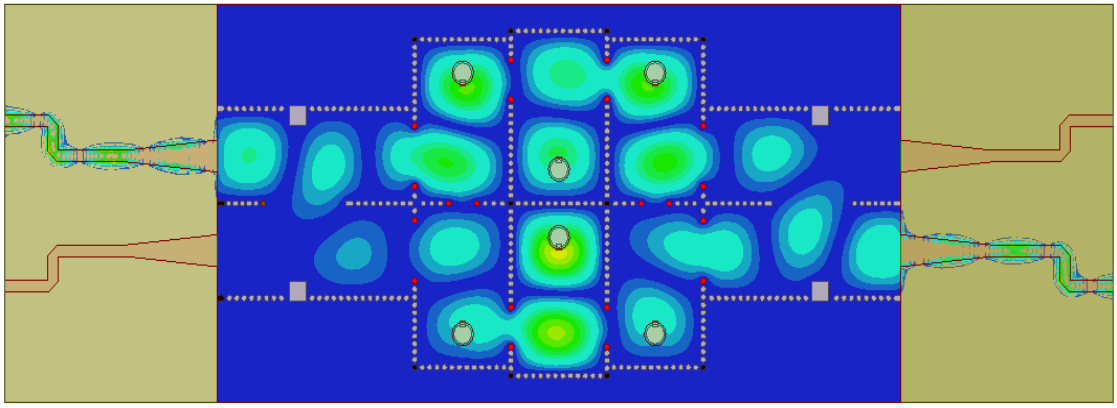

Figure 3-28 Simulation of the improved HCFM with total of six tuning elements

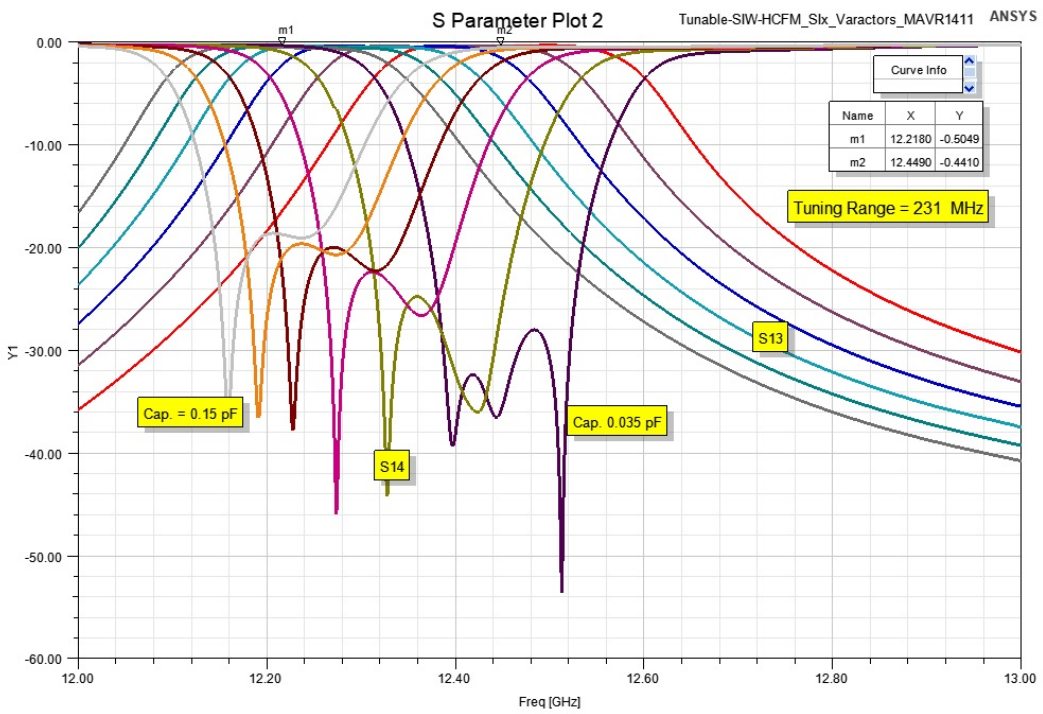

Figure 3-29 S-parameters of the improved model of SIW HCFM with six tuning elements

3.4 Measurement results

This section presents the measurement results of the SIW bandpass filters and compact improved HCFM using SIW. The SIW filters and HCFM are designed following the same procedure presented in this thesis. The simulation and measurement results are compared and discussed.

3.4.1 SIW bandpass filters

A number of SIW bandpass filters are first fabricated and tested for verification purpose.

A picture of fabricated SIW bandpass filter with a center frequency of 12.08 GHz and fractional bandwidth of 4.4% is shown in Figure 3-30. The filter is fabricated using RT/Duroid 6002, with dielectric constant ε_r = 2.9, L_{siw}=0.719 in, W_{siw}=0.452 in, radius of metallic vias of 0.013 in and distance between two adjacent vias of 0.041 in.

The simulation and measurement results are shown in Figure 3-31. The results show a shift of the operational frequency of the fabricated filter. The operational frequency of the SIW filter is controlled by design parameters, such as L_{siw}, W_{siw} and the size of the vias. In addition, the dielectric constant of the substrate material has significant effect on center frequency of the filter.

In order to analyze and better understand the mismatch between measurement and simulated results, the variance in substrate's dielectric constant ε_r is simulated in HFSS. The simulation results for the changes in dielectric constant on the operational frequency of the filter are shown in Figure 3-22, showing a similar shift as observed in the measurement results. It is therefore concluded that ε_r = 2.82 is closer to the actual dielectric

constant of the material. Figure 3-33 presents the measurement and simulation results using the adjusted dielectric constant of ε_r = 2.82. It can be seen that the measurement and simulation results are in better agreement.

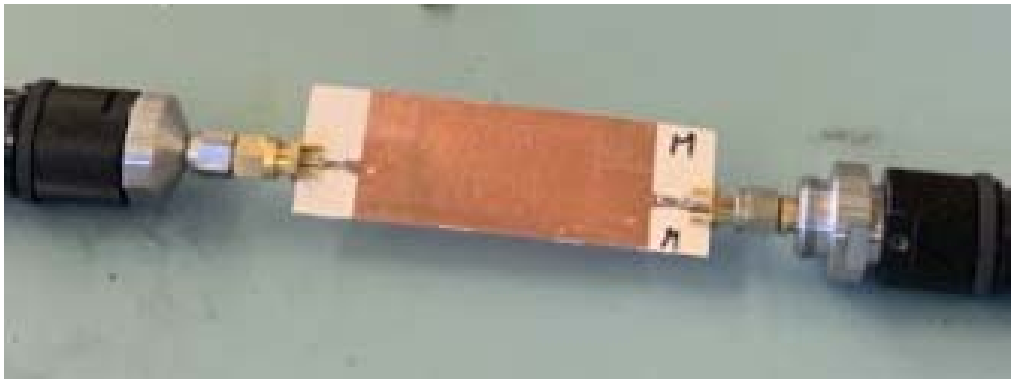

Figure 3-30 Photograph of fabricated SIW bandpass filter operating at 12.08 GHz

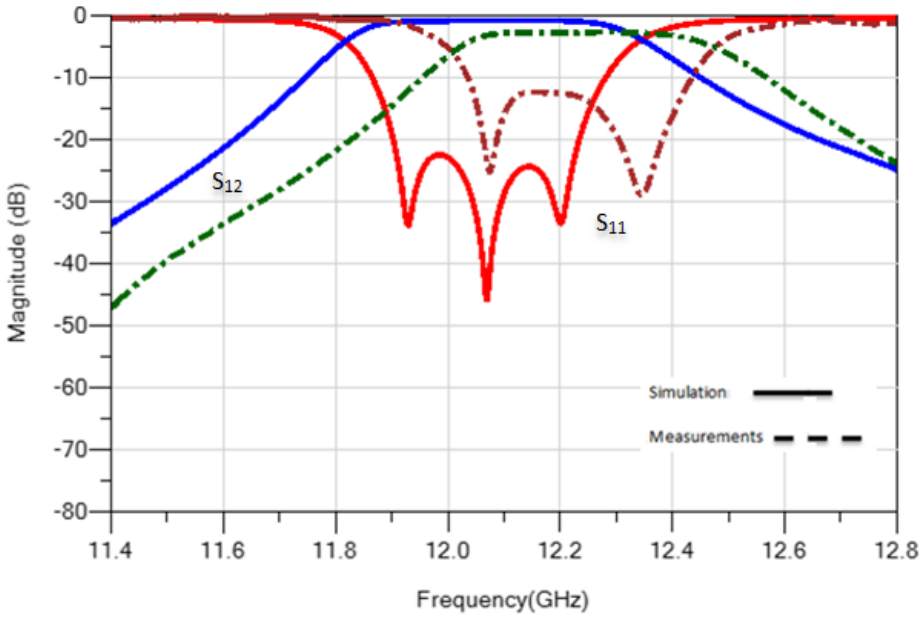

Figure 3-31 |S11| and |S12| of the SIW filter (12.08 GHz)

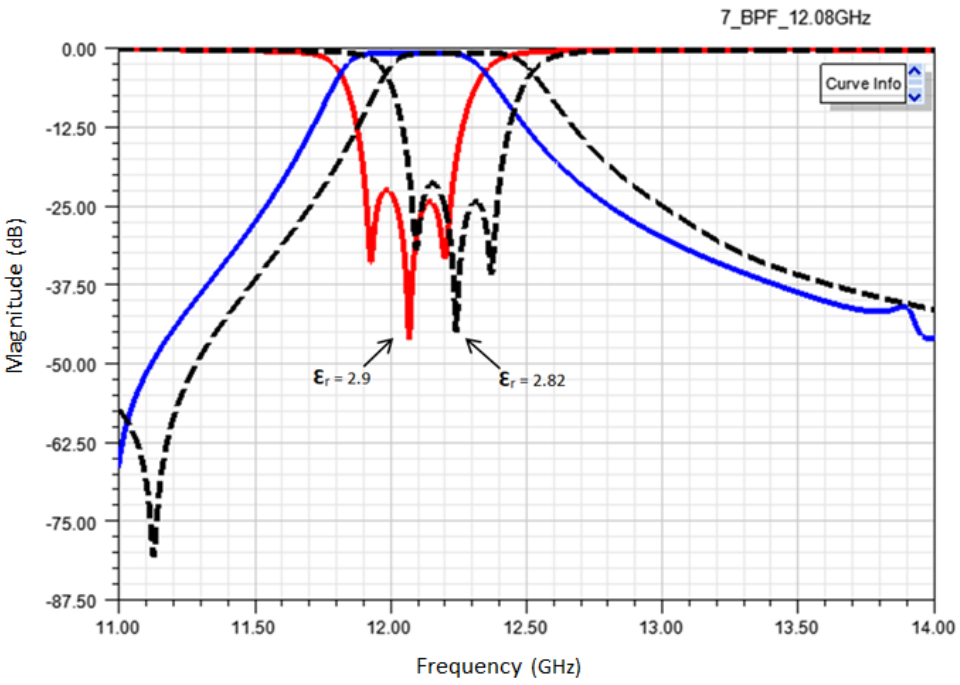

Figure 3-32 Effect of changes in dielectric constant of the substrate

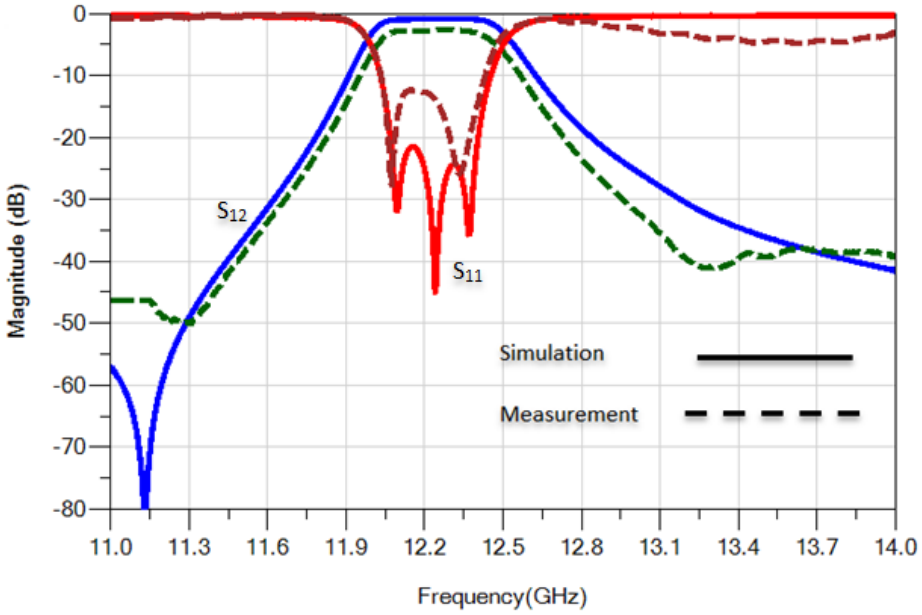

Figure 3-33 S-parameter of the SIW bandpass filter (12.08 GHz) with adjusted dielectric constant

Another SIW bandpass filter with center frequency of 12.56 GHz and fractional bandwidth 4.4% is shown in Figure 3-34. The filter is fabricated using the same dielectric material, and L_{siw}=0.68 in, W_{siw}=0.452 in, radius of metallic vias of 0.013 in and distance between two adjacent vias of 0.041 in.

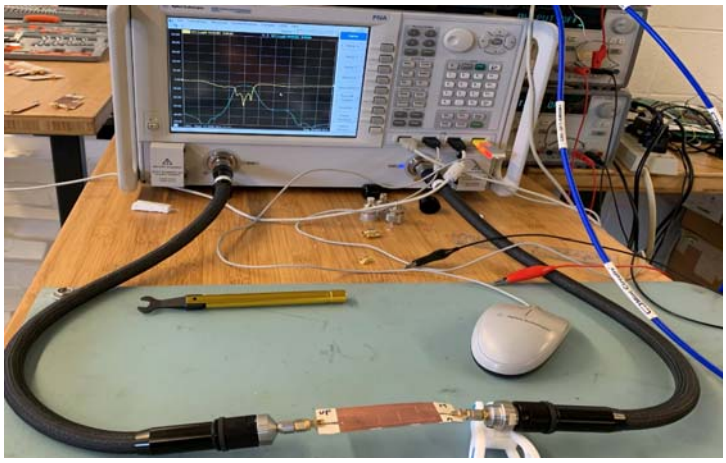

Figure 3-34 Measurement of the fabricated SIW bandpass filter operating at 12.56 GHz

Figure 3-35 shows the measurement and simulation results of the SIW bandpass filter. As discussed in previous section, the simulation using the adjusted dielectric constant of ε_r = 2.82 shows good agreement with the measurement. The return loss $|S_{11}|$ remains blow -14 dB and $|S_{12}|$ indicates a bandwidth reduction, which is expected to be caused by fabrication tolerances.

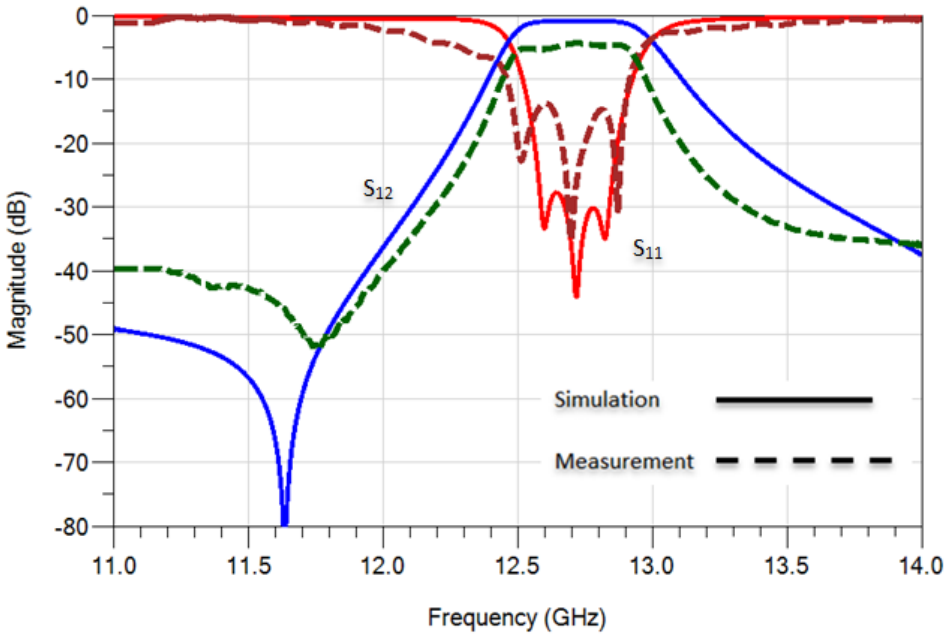

Figure 3-35 S-parameter of the SIW bandpass filter (12.56 GHz) with adjusted dielectric constant

3.4.2 Improved HCFM using SIW

Figure 3-36 shows the fabricated improved HCFM using SIW technology. The HCFM comprises of two identical bandpass filter and the reduced quadrature hybrid couplers. The HCFM operates at 12.32 GHz with bandwidth of 500 MHz and is fabricated using RT/Duroid 6002, with dielectric constant $\varepsilon_r = 2.9$, $L_{siw} = 0.693$ in, $W_{siw} = 0.452$ in, radius of metallic vias of 0.013 in and distance between two adjacent vias of 0.041 in.

The measured $|S_{13}|$ of the fabricated HCFM and simulation results using HFSS are shown in Figure 3-37. Similar frequency misalignment between the simulation and measurement results is observed when the nominal value of $\varepsilon_r = 2.9$ is used in the simulation. The design is then simulated in HFSS using adjusted dielectric constant of $\varepsilon_r = 2.82$. Results are compared with measurement in Figure 3-38, showing improved agreement. The $|S_{11}|$ and

$|S_{12}|$ are below -10 dB for the entire frequency range of interest. The differences between simulation and measurement are expected to be caused by fabrication tolerances.

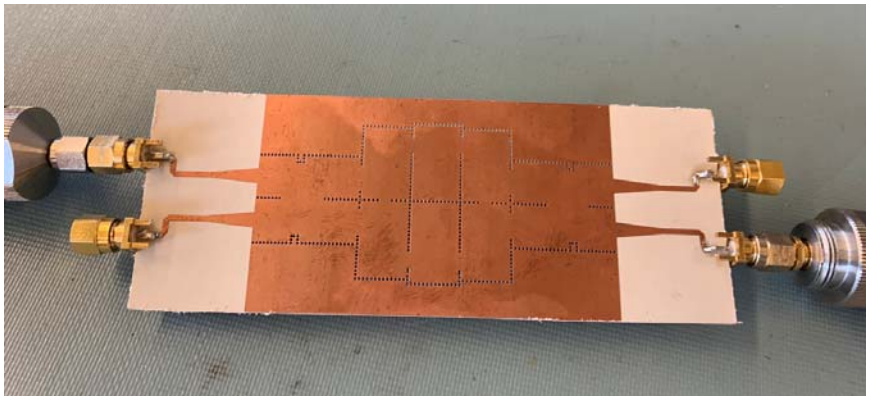

Figure 3-36 Photograph of fabricated improved HCFM using SIW

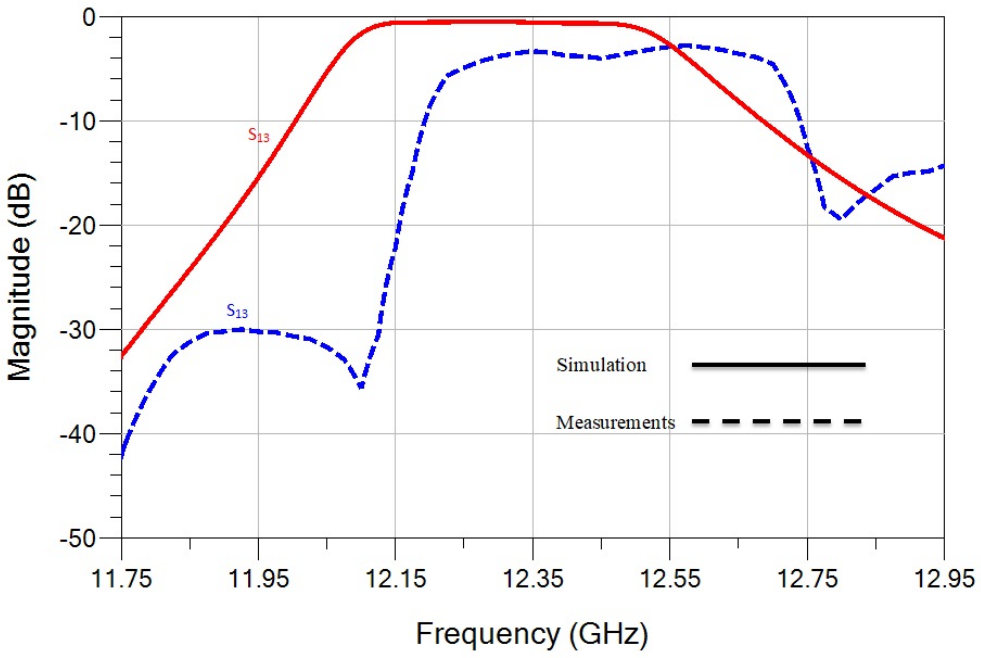

Figure 3-37 Simulation (ε_r = 2.9) and measurement of $|S_{13}|$ of the improved HCFM

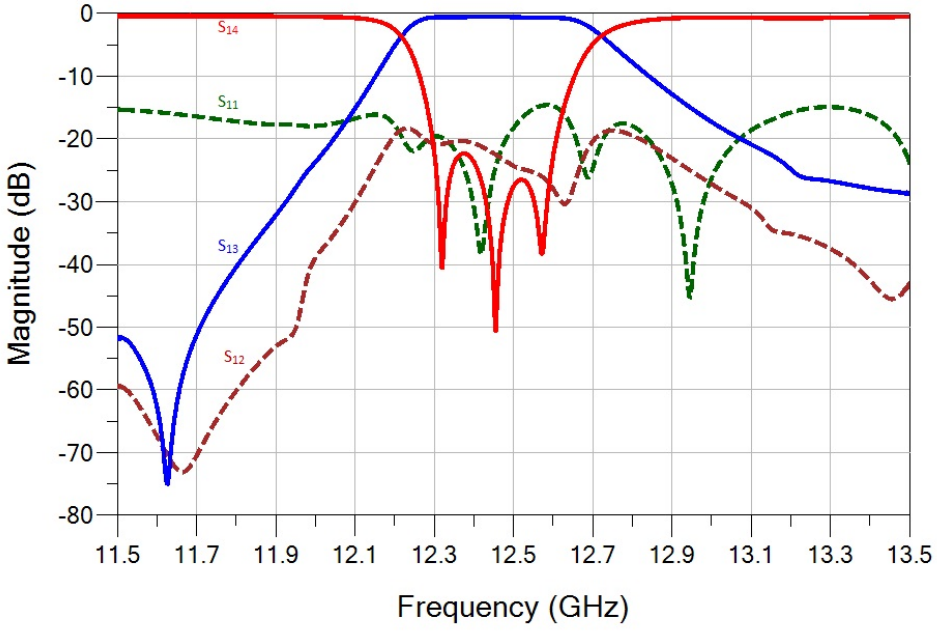

(a)

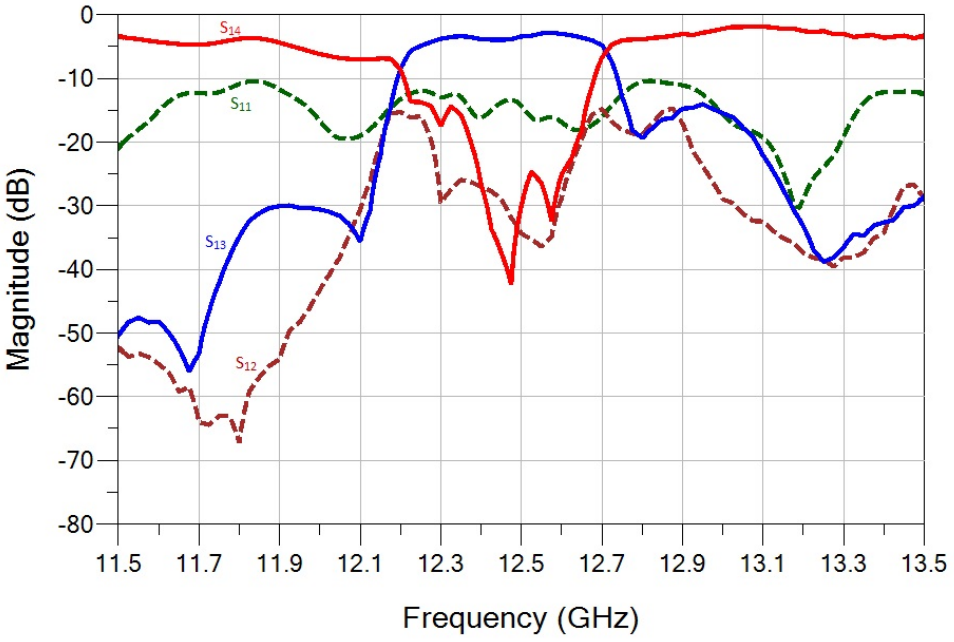

(b)

Figure 3-38 S-parameter of improved HCFM: (a) simulation and (b)measurement

3.5 Summary

This chapter presents the design of the improved HCFM using SIW technology. The design process is thoroughly described. As demonstrated, the proposed design of HCFM using SIW achieves significant reduction in size comparing to other designs.

The feasibility of electronic tuning of multiplexers is also investigated in this chapter. First the tuning of an SIW cavity resonator using one varactor diode is simulated on single SIW cavity, resulting in 460 MHz tuning range. Next it is shown that when two varactor diodes are used the tuning range is improved to 610 MHz. Furthermore, the tuning method is applied to the SIW HCFM and successfully achieves 230 MHz of tuning range.

Finally, the compact improved HCFM using SIW is validated using measurement results. The SIW HCFM, together with two SIW bandpass filters, is fabricated and tested. The frequency misalignment between the simulation and measurement results is investigated. The dielectric constant ε_r is subsequently adjusted from the nominal value of 2.9 to 2.82, resulting in good agreement with simulation results.

Chapter 4

Tunable Diplexer

4.1 Tunable diplexer by cascading a bandpass filter with the HCFM

Communication industry using multiplexers as combiners and channelizers for more than four decades [2]. Diplexers are a form of multiplexer with two distinct channels. The interaction between the two channels of a diplexer makes the design of a tunable diplexer more challenging comparing to the design of a tunable filter.

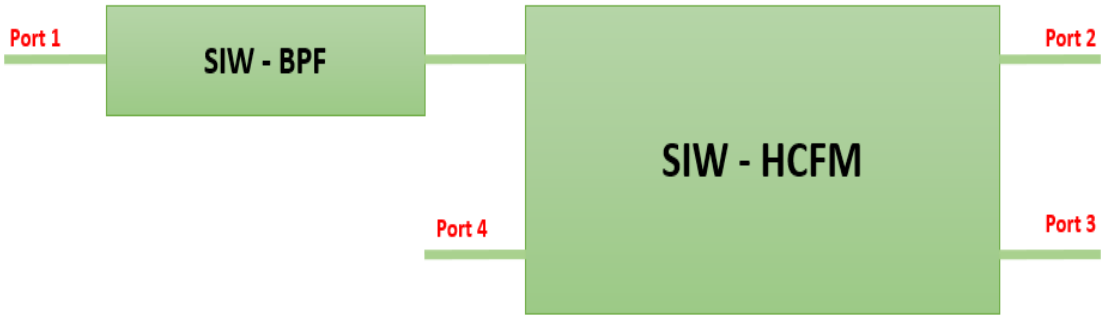

Figure 4-1 Diplexer formed by cascading bandpass filter and HCFM

This thesis presents a novel methodology for tunable substrate integrated waveguide (SIW) diplexer by combining an SIW bandpass filter (BPF) with the improved hybrid-coupled filter module (HCFM) developed in the previous chapter. Reduction of footprint, simplicity of tuning process, and different applications of the cascaded system are important advantages for the diplexer presented in this thesis. The proposed topology is shown in Figure 4-1, cascading a bandpass filter with the HCFM.

As discussed in Chapter 3, the center frequencies of a bandpass filter can be readily tuned for both an SIW filter and an HCFM. Tuning of the bandwidth of a filter can be more complex. For a tunable diplexer, both center frequency and bandwidth should be adjustable, which is even more difficult. In the following sections, it will be shown that the topology in Figure 4-1 enables the realization of tunable diplexer, with both tunable center frequency and bandwidth. This can be achieved by simply tuning the center frequencies of the bandpass filter and/or the HCFM, without tuning the bandwidth of either.

In order to demonstrate the idea of tunable SIW diplexer, assume the system in Figure 4-1 cascades a five poles bandpass filter with an HCFM. The center frequency of the five-pole filter is assumed to have a tuning range of less than 460 MHz. Figure 4-2 shows the S-parameters of the five poles bandpass filter when the center frequency is 12350 MHz, with a fractional bandwidth of 3.25%. The HCFM's center frequency has a tuning range of less than 230 MHz. Figure 4-3 shows the S-parameters of the HCFM when the center frequency is 12500 MHz, with fractional bandwidth of 1.3%.

Note that the cases shown in the following sections assume only tuning of center frequencies of bandpass filter and/or HCFM. If both center frequencies and bandwidth are tunable, it is evident that even greater tuning flexibility for the tunable diplexer can be achieved.

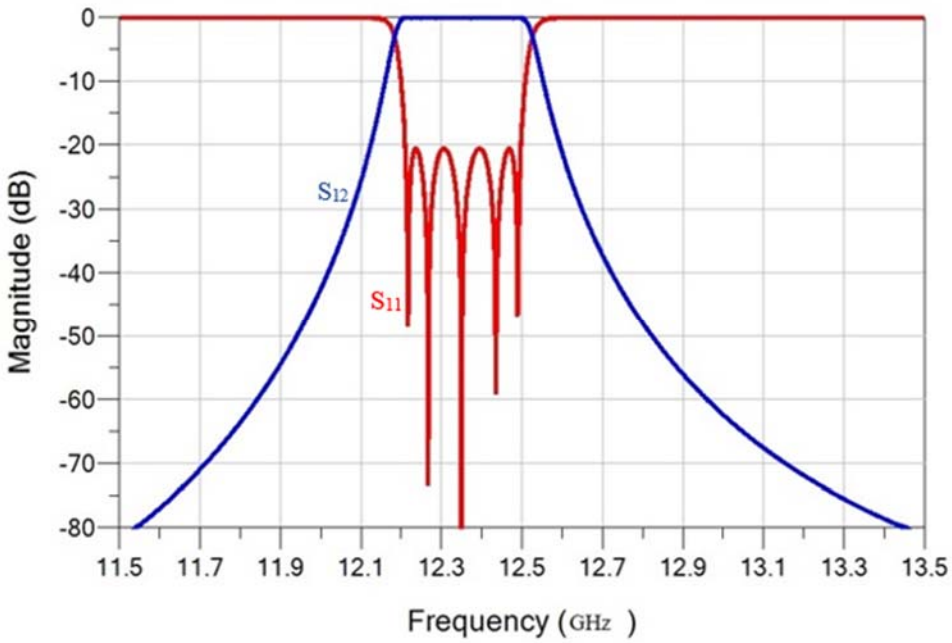

Figure 4-2 Five poles bandpass filter

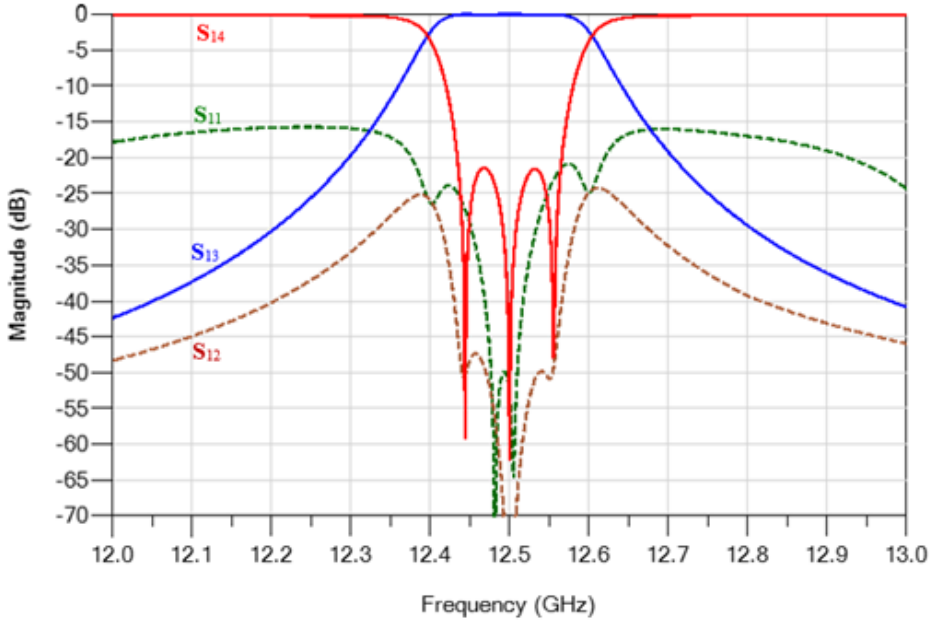

Figure 4-3 Improved HCFM operating at 12500 MHz

4.1.1 Effect of tuning the center frequency of the bandpass filter only

The first scenario to be investigated in the combination of bandpass filter with the improved HCFM is when the bandpass filter is tunable and HCFM remains unchanged with a constant center frequency and bandwidth.

The bandpass filter operating at center frequency f_0 = 12300 MHz has a bandwidth of 400 MHz, while the HCFM is centered at 12500 MHz with 160 MHz bandwidth, as shown in Table 4-1 case (a). This results in the diplexer comprising of two distinct channels (blue and red) shown in Figure 4-4(a). $|S_{11}|$ remains below -12 dB for both channels for the entire bandwidth, and $|S_{14}|$ around 12600 MHz is lower than -25 dB.

Table 4-1 Center frequency f_0 and bandwidth (BW) of the HCFM and BPF with f_0 of BPF lower than f_0 of HCFM

	HCFM		BPF	
	f_0 (MHz)	BW (MHZ)	f_0 (MHz)	BW (MHZ)
Case (a)	12500	160	**12300**	400
Case (b)	12500	160	**12350**	400

Next, tuning only the center frequency f_0 of the bandpass filter to 12350 MHz, while the center frequency of the HCFM is kept unchanged as in Table 4-1, case (b), the diplexer's S-parameter are changed as shown in Figure 4-4(b). The diplexer still has two distinct channels (blue & red), with wider bandwidth for the upper channel (blue curve) and narrower bandwidth for the lower channel (red curve) comparing to Figure 4-4(a). Thus, the bandwidths of the diplexer channels are tuned by changing only the center frequency of the bandpass filter. $|S_{11}|$ remains below -12 dB for both channels for the entire bandwidth. $|S_{14}|$ around 12600 MHz is lower than -15 dB. Note that as the center frequency of the bandpass filter moves closer to that of the HCFM, $|S_{14}|$ around 12600 MHz increases.

If rejection less than 15 dB is acceptable, the center frequency of the bandpass filter can be tuned to even higher.

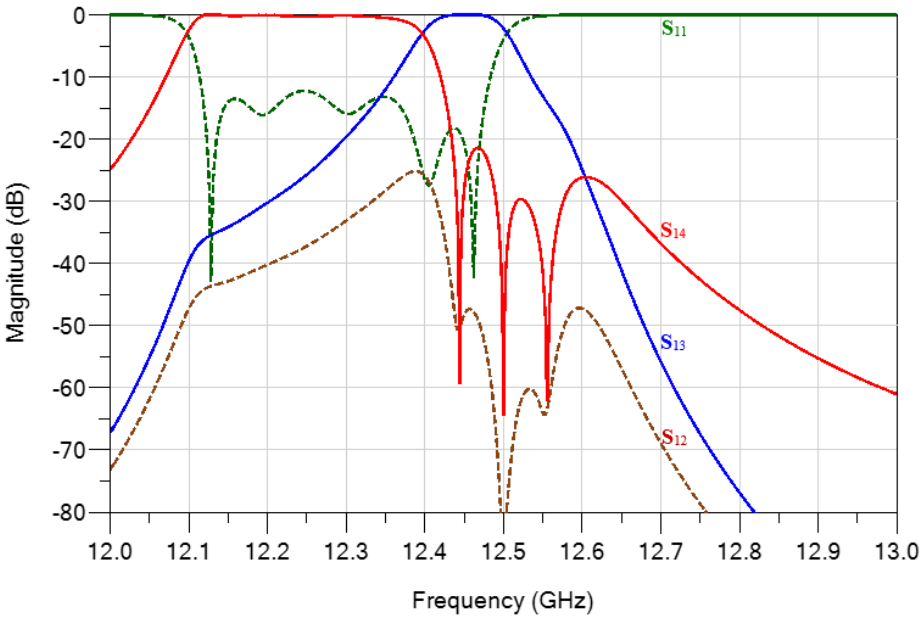

(a)

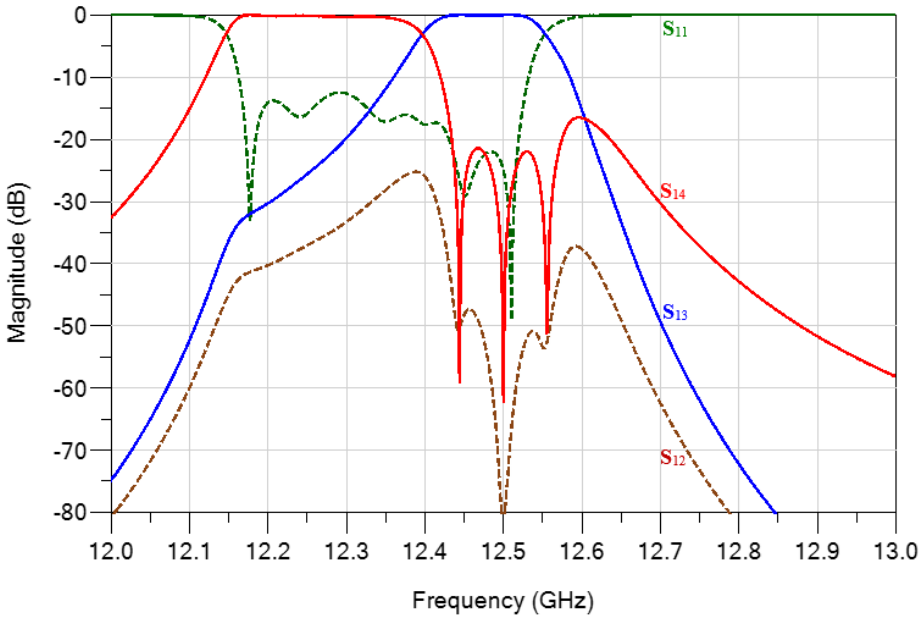

(b)

Figure 4-4 Tunable diplexer in accordance with Table4-1

Table 4-2 Center frequency f_0 and bandwidth (BW) of the HCFM and BPF with f_0 of BPF higher than f_0 of HCFM

	HCFM		BPF	
	f_0 (MHz)	BW (MHZ)	f_0 (MHz)	BW (MHZ)
Case (a)	12500	160	**12700**	400
Case (b)	12500	160	**12650**	400

Table 4-2 shows another two cases, when the center frequency f_0 of the bandpass filter is higher than that of the HCFM and only f_0 of the bandpass filter is changed in both cases. The center frequency of the bandpass filter is tuned to 12700 MHz in case (a), and the diplexer new results are shown in Figure 4-5(a), where the diplexer still has two distinct channels (blue and red). The upper channel's center frequency is much higher comparing to the previous two cases. $|S_{11}|$ is below -15 dB for both channels and $|S_{14}|$ around 12400 MHz remains below -25 dB.

Finally the center frequency of the bandpass filter is changed to 12650 MHz, case (b), and the diplexer results are shown in Figure 4-5(b). The results show $|S_{11}|$ for the entire bandwidth remains below -15 dB for both channels and $|S_{14}|$ around 12400 MHz is below -15 dB. Similar to case (b) of Table 4-1, as the center frequency of the bandpass filter moves closer to that of the HCFM, $|S_{14}|$ around 12400 MHz increases. If rejection less than 15 dB is acceptable, the center frequency of the bandpass filter can be tuned to even lower.

In summary by tuning only the center frequency of the five poles bandpass filter from 12300 MHz to 12700 MHz, while the operational frequency of the HCFM has been kept constant, the tunable diplexer with two distinct channels was generated.

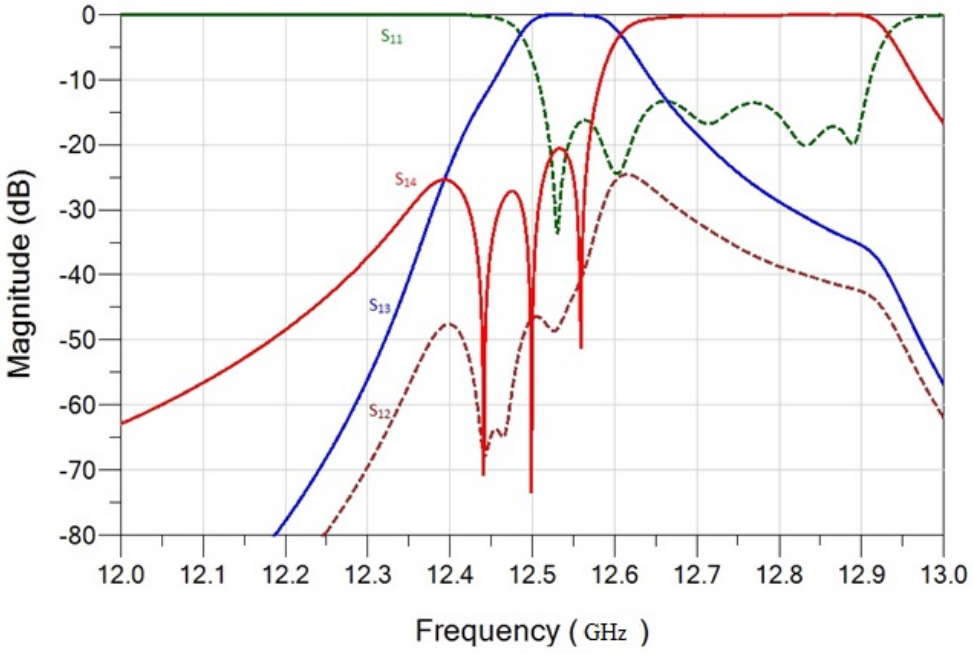

(a)

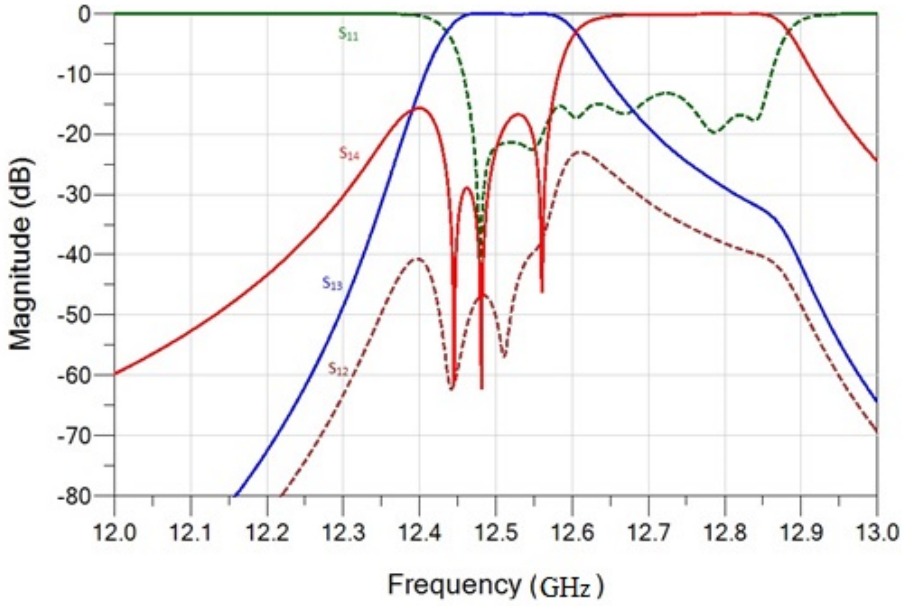

(b)

Figure 4-5 Tunable diplexer in accordance with Table 4-2

4.1.2 Effect of tuning the center frequency of the HCFM

The second scenario to be considered is to have a tunable diplexer only by tuning the center frequency of the HCFM.

Table 4-3 shows the center frequency f_0 and bandwidth of the bandpass filter and HCFM, with f_0 of the bandpass filter lower than that of the HCFM. The bandpass filter operating at center frequency f_0 = 12300 MHz has a bandwidth of 400 MHz, while the HCFM with 160 MHz bandwidth is tuned to 12480 MHz in case (a) and 12550 MHz in case (b), respectively. The results are shown in Figure 4-6(a) and (b). $|S_{11}|$ remains below -15 dB and $|S_{14}|$ around 12600 MHz is below -15 dB for both channels.

As the HCFM's center frequency is shifted away from the bandpass filter, the bandwidth of the lower frequency channel becomes wider and the bandwidth of the higher frequency channel becomes narrower. As seen in Figure 4-6(a), when the HCFM's center frequency is shifted closer to the bandpass filter, the out-of-band rejection of the lower frequency channel becomes worse around 12600 MHz. If less rejection can be accepted, the HCFM's center frequency can be further reduced.

Table 4-3 Center frequency f_0 and bandwidth (BW) of the HCFM and BPF with f_0 of HCFM higher than f_0 of BPF

	HCFM		BPF	
	f_0 (MHz)	BW (MHZ)	f_0 (MHz)	BW (MHZ)
Case (a)	**12480**	160	12300	400
Case (b)	**12550**	160	12300	400

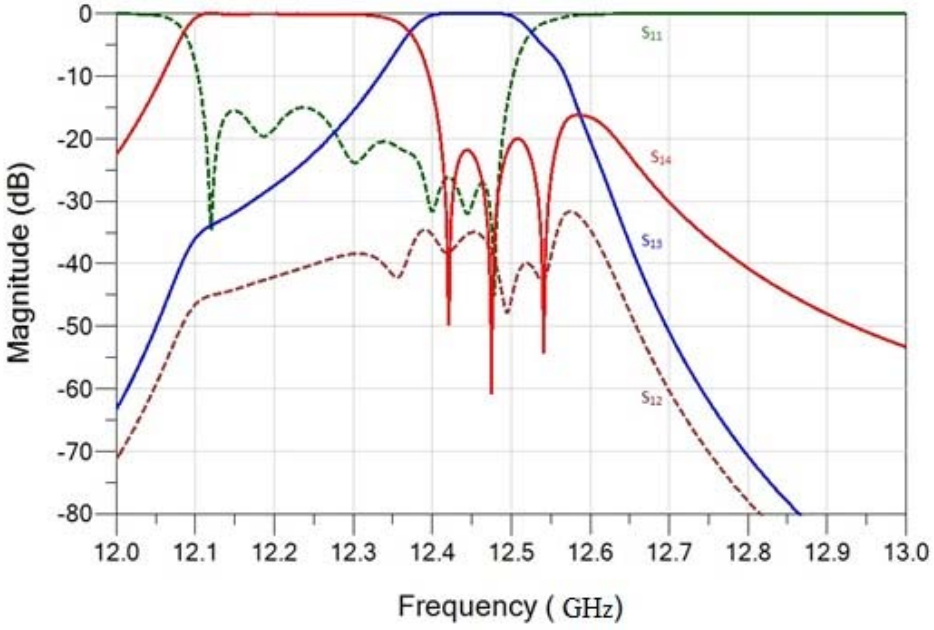

(a)

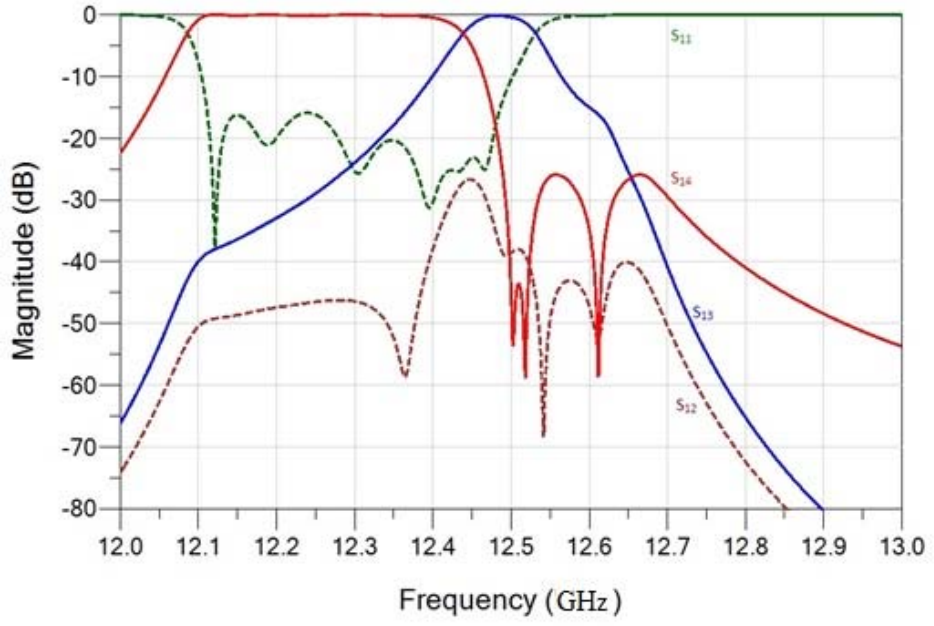

(b)

Figure 4-6 Tunable diplexer in accordance with table 4-3

Next the bandpass filter's center frequency is changed to 12700 MHz, which is above the center frequency of the HCFM. The center frequency of the HCFM varies from 12480 MHz to 12550 MHz, as shown in Table 4-4.

The S-parameters are shown in Figure 4-7(a) and Figure 4-7(b), demonstrating successful tunability of the diplexer. $|S_{11}|$ remains below -12 dB for both channels. Similar to previous cases, when the HCFM's center frequency is closer to that of the bandpass filter, the out-of-band rejection of the higher frequency channel becomes worse around 12450 MHz. If less rejection can be accepted, the HCFM's center frequency can be further increased.

Table 4-4 Center frequency f_0 and bandwidth (BW) of the HCFM and BPF with f_0 of HCFM lower than f_0 of BPF

	HCFM		BPF	
	f_0 (MHz)	BW (MHZ)	f_0 (MHz)	BW (MHZ)
Case (a)	**12480**	160	12700	400
Case (b)	**12550**	160	12700	400

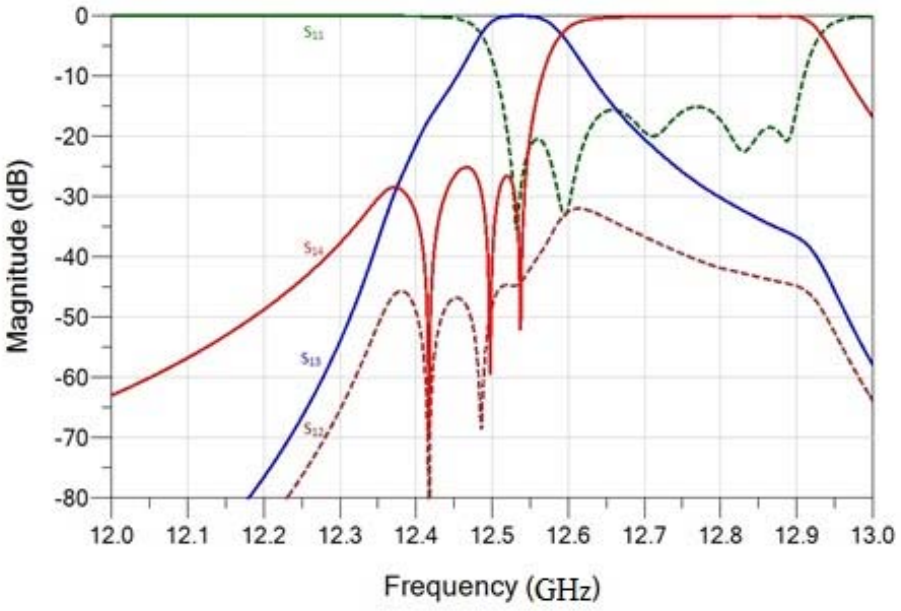

(a)

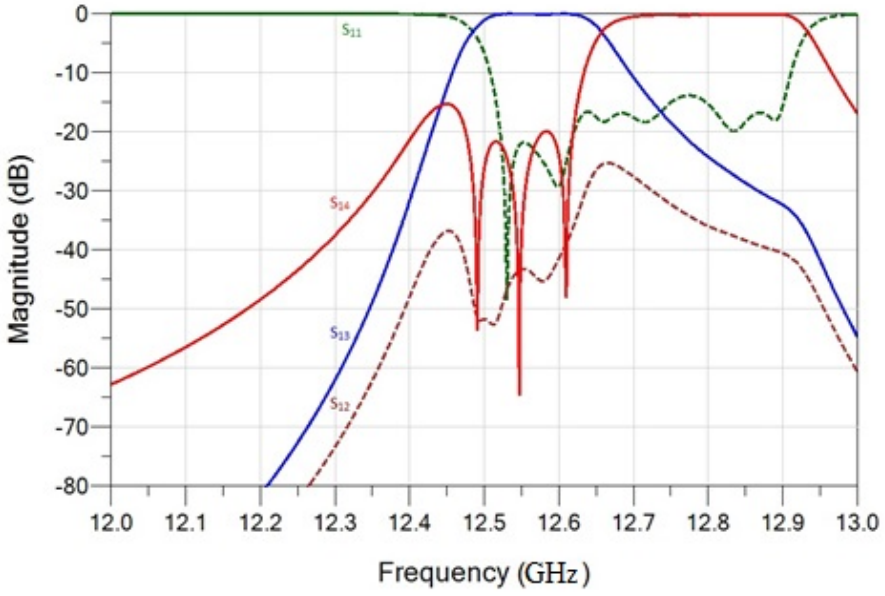

(b)

Figure 4-7 Results of tunable diplexer in accordance with Table 4-4

4.1.3 Tunable diplexer with one channel having dual passband

The last scenario considered herein is to have one of the diplexer channels with dual passband. This happens when the center frequency of the HCFM is within the passband of the bandpass filter and the bandwidth of the HCFM is smaller than that of the bandpass filter, as the two cases in Table 4-5.

Figure 4-8 shows the S-parameters of the diplexer with one channel having dual passband. By changing the center frequency of the bandpass filter, the passbands of the channel can be easily adjusted, as shown in Figure 4-8(a) and (b). When the center frequency of the bandpass filter increases, the passband on the low frequency side reduces, while the passband on the high frequency side increases. $|S_{11}|$ remains below -15 dB for both channels.

Table 4-5 Center frequency f_0 and bandwidth (BW) of the HCFM and BPF with passband of HCFM within that of BPF

	HCFM		BPF	
	f_0 (MHz)	BW (MHZ)	f_0 (MHz)	BW (MHZ)
Case (a)	12500	160	**12500**	400
Case (b)	12500	160	**12550**	400

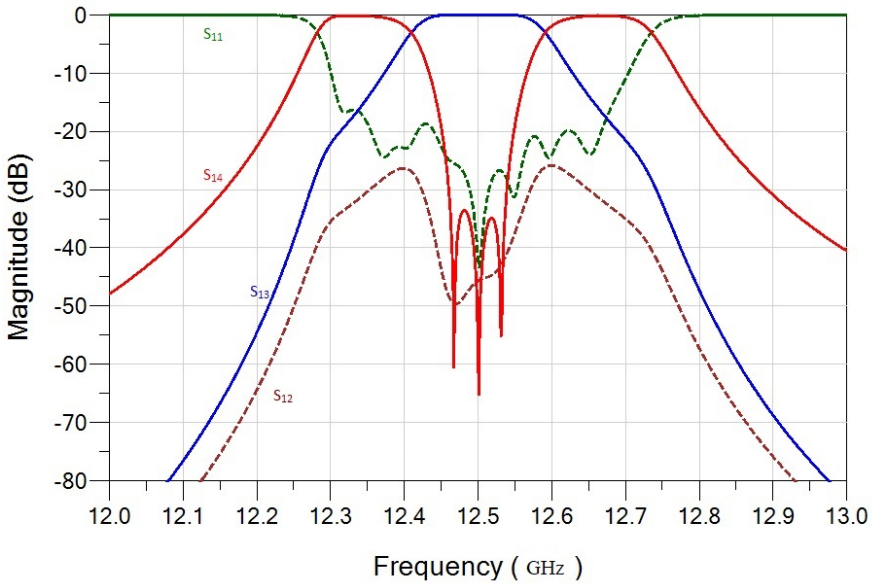

(a)

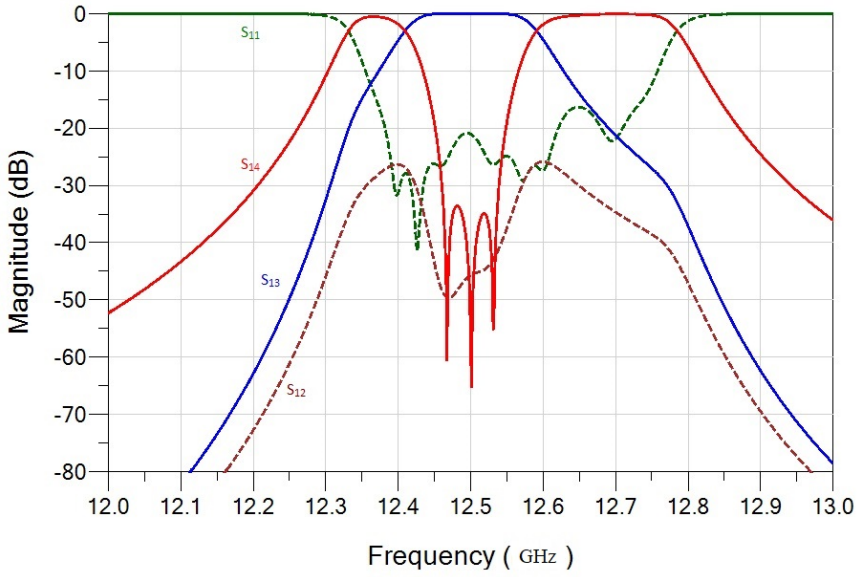

(b)

Figure 4-8 Results of tunable diplexer in accordance with Table 4-5

4.2 Measurement results

Different scenarios for the tunable diplexer have been discussed in previous section, using the simulation of the diplexer's circuit model in ADS. In order to experimentally prove the idea of tunable diplexer, the two structures of low profile SIW diplexers shown in Figure 4-9 are fabricated. Each diplexer is comprised of an SIW three-pole bandpass filter cascaded with an SIW HCFM. For the first diplexer, the bandpass filter has a center frequency of 12.1 GHz and a bandwidth of 560 MHz. In the second diplexer, the bandpass filter has a center frequency of 12.55 GHz and similar bandwidth as in the first diplexer. In both cases, the HCFM has a center frequency of 12.32 GHz and a bandwidth of 500 MHz. The substrate is RT/duroid-6002 with thickness of 0.02 in. The adjusted dielectric constant of $\varepsilon_r = 2.82$ is assumed in the design process.

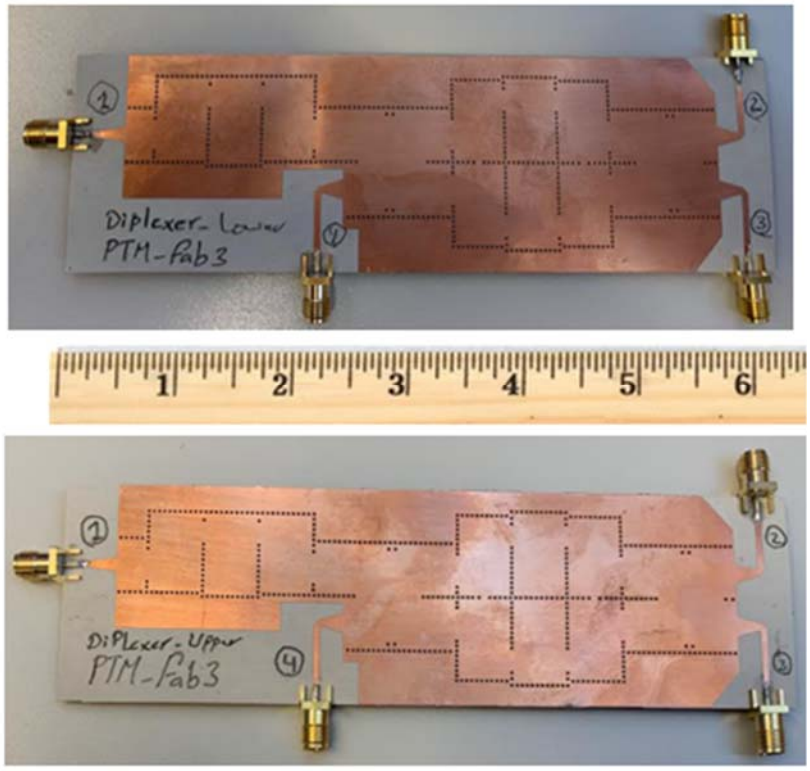

Figure 4-9 Photograph of fabricated SIW diplexers

A two-port network analyzer is used for measurement. As shown in Figure 4-10 two ports of the four-port design are connected to a network analyzer and 50 Ω matched loads are used for the rest of the ports.

Measurement results and full wave EM simulations are shown in Figure 4-11 and Figure 4-12 for the two diplexers, respectively. As expected, the resulting two diplexers have different center frequencies and bandwidths. Relatively good agreement between EM simulations and measurements can be observed in both cases, validating the concept of tunable diplexer by varying only the center frequency of the bandpass filter. The differences between simulation and measurement results are expected to be caused by fabrication tolerances.

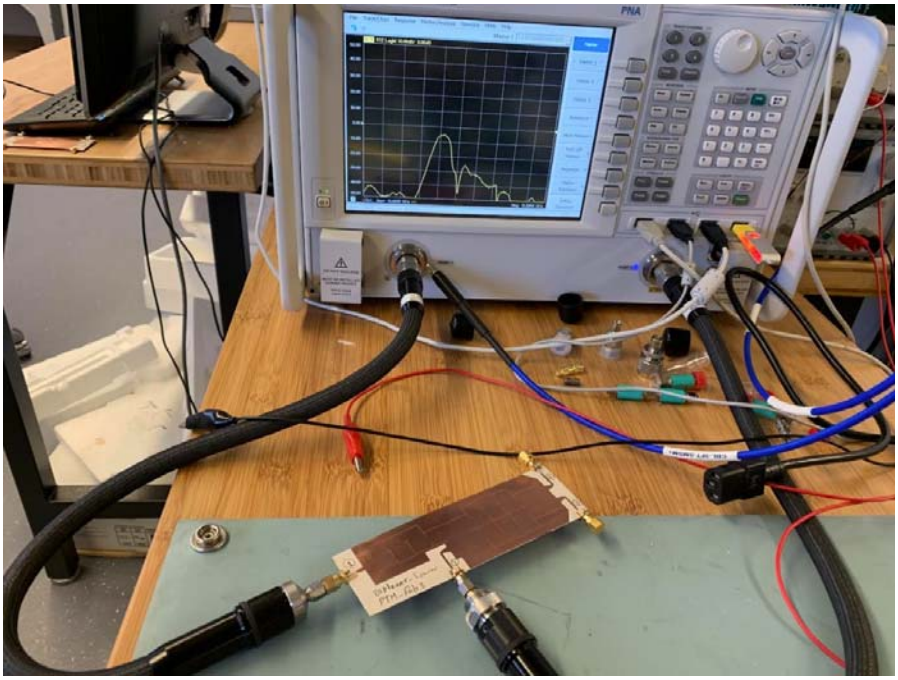

Figure 4-10 Measurement setup of the diplexer using network analyzer

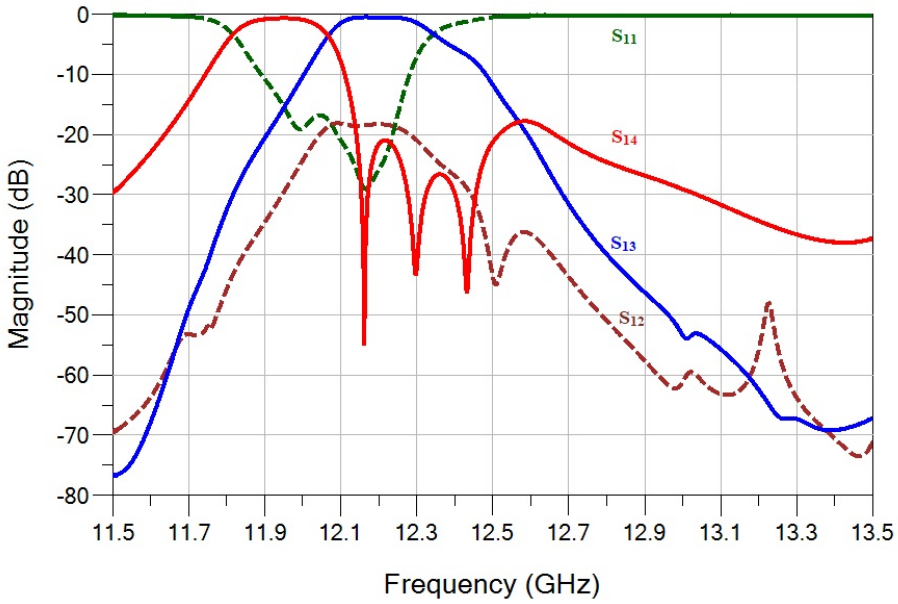

(a)

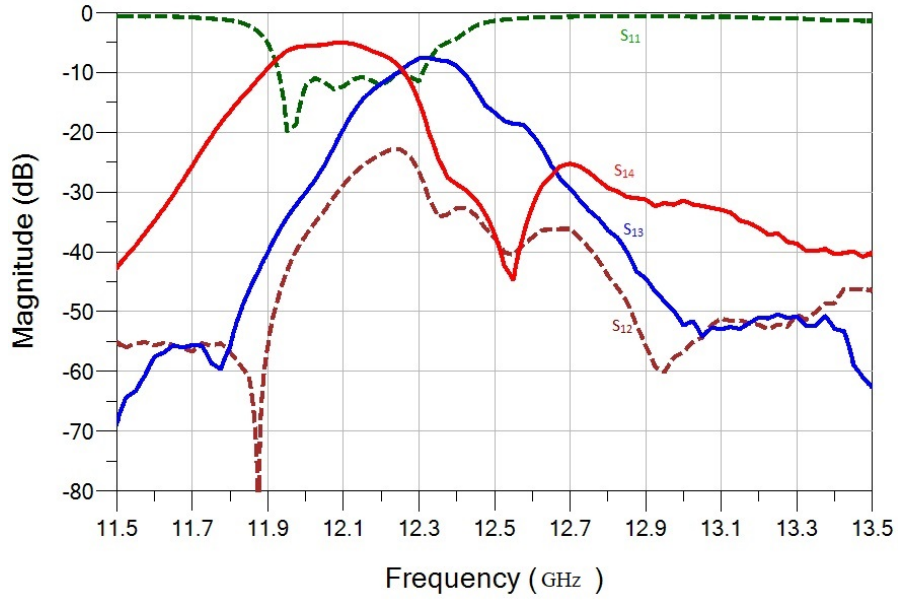

(a)

Figure 4-11 (a) EM simulation and (b) measurement results of the diplexer when the center frequency of the bandpass filter is 12.1 GHz

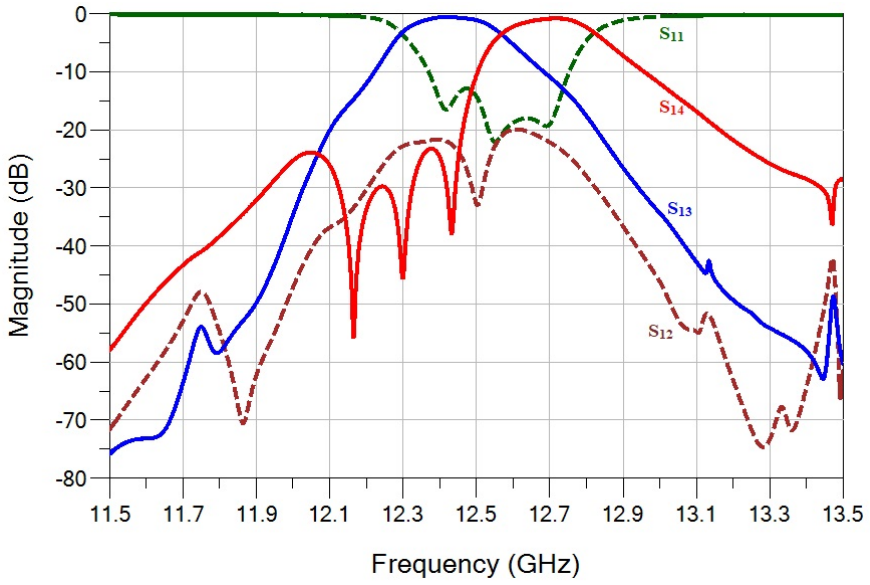

(a)

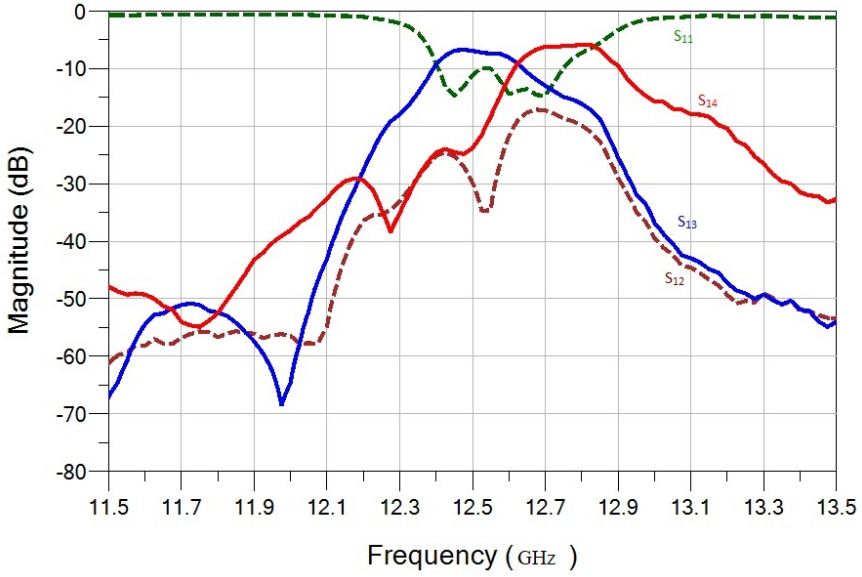

(b)

Figure 4-12 (a) EM simulation and (b) measurement results of the diplexer when the center frequency of the bandpass filter is 12.55 GHz

4.3 Summary

This chapter presents a novel method for implementing tunable SIW diplexer by cascading an SIW bandpass filter with the improved HCFM. Different possibilities of tunable diplexer using the cascaded system have been discussed. As demonstrated, tunability of diplexer channels has been successfully accomplished. Specifically, both center frequencies and bandwidths of the diplexer channels can be adjusted by simply tuning the center frequency of the bandpass filter and/or by tuning the center frequency of the HCFM.

Finally, for proof of concept, two cascaded designs are fabricated with only the center frequencies of the bandpass filters being different, resulting in two diplexers with different channels. Good agreement is seen between EM simulations and measurement results for both designs, validating the concept of the new tunable diplexer.

Chapter 5

Conclusion and Future Work

In this era of modern communication network systems, there has been increasing need for multipurpose and multifunctional devices. Features such as being compact in size, tunable in frequency and bandwidth, and low in cost are among highly demanded characterizations of microwave components.

In this thesis, a compact design of the improved hybrid-coupled filter combiner (HCFM) using substrate integrated waveguide (SIW) technology is successfully developed. The proposed SIW HCFM achieves 60% footprint reduction comparing to the improved HCFM implemented using conventional rectangular waveguide. The feasibility of electronic tuning of the HCFM is also investigated. Simulations of an SIW cavity resonator using one varactor diode show 460 MHz tuning range. It is also shown that when two varactor diodes are used the tuning range is improved to 610 MHz. The tuning method is then applied to the SIW HCFM and successfully achieves 230 MHz of tuning range. In additions, the compact improved HCFM using SIW is validated using measurement results. The frequency misalignment between the simulation and measurement results is investigated using fabricated SIW filters. Good agreement between simulation and measurement results is achieved for the designed HCFM.

Moreover, a new methodology is developed for tunable diplexer. Microwave diplexers have been widely employed in communication systems. The tunable diplexer is formed by combining a bandpass filter with the improved HCFM. Tunability of the diplexer is

investigated through simulations by considering different scenarios. By simply tuning the center frequency of the bandpass filter and/or the HCFM, both center frequencies and bandwidths of the diplexer channels can be adjusted. If both center frequencies and bandwidth are tunable for the bandpass filter and/or the HCFM, even greater tuning flexibility for the tunable diplexer can be expected. The concept is next validated through measurement results. Two designs are fabricated. Only the center frequencies of the bandpass filters in the cascaded systems are different, and the HCFM remains the same in the two designs. As expected, the resulting two diplexers have different center frequencies and bandwidths for each channel. Measurements results agree well with EM simulations for both designs.

The following ideas can be investigated further for future work:

- Fabrication of the electronically tuned SIW cavity resonator to verify experimentally the effect of single and double varactor diodes;
- Further investigation of achieving wider range of electronic tuning of SIW structure;
- Fabrication and measurement of the SIW HCFM loaded with varactor diodes; and
- Further investigation and verification of electronically tunable diplexers.

References

[1] R. J. Cameron, C. M. Kudsia, and R. R. Mansour, *Microwave Filters for Communication Systems: Fundamentals, Design, and Applications*. Hoboken, NJ: Wiley-Interscience, 2007.

[2] Y. Sun, Compact Microwave Filter Designs based on Cavity Resonators, MASc Thesis, University of Ontario Institute of Technology, 2016.

[3] L. Zhu, R. R. Mansour and M. Yu, "A compact waveguide diplexer employing dual-band resonators," *2014 IEEE MTT-S International Microwave Symposium (IMS2014)*, Tampa, FL, 2014.

[4] L. Zhu, R. R. Mansour and M. Yu, "Compact Waveguide Dual-Band Filters and Diplexers," in *IEEE Transactions on Microwave Theory and Techniques*, vol. 65, no. 5, pp. 1525-1533, May 2017.

[5] S. Bastioli, L. Marcaccioli and R. Sorrentino, "An original resonant Y-junction for compact waveguide diplexers," 2009 *IEEE MTT-S International Microwave Symposium Digest*, Boston, MA, 2009.

[6] Y. Cheng, W. Hong and K. Wu, "Investigation on Tolerances of Substrate Integrated Waveguide (SIW)," 2007 *Asia-Pacific Microwave Conference*, Bangkok, 2007.

[7] S. S. Sabri, B. H. Ahmad and A. R. B. Othman, "A review of Substrate Integrated Waveguide (SIW) bandpass filter based on different method and design," 2012 *IEEE Asia-Pacific Conference on Applied Electromagnetics (APACE)*, Melaka, 2012.

[8] E. Díaz-Caballero, Á. Belenguer, H. Esteban, V. E. Boria, C. Bachiller and J. V. Morro, "Analysis and design of passive microwave components in substrate integrated waveguide technology," 2015 *IEEE MTT-S International Conference on Numerical Electromagnetic and Multiphysics Modeling and Optimization (NEMO)*, Ottawa, ON, 2015.

[9] Y. J. Cheng, *Substrate Integrated Antennas and Arrays*. 1st ed. Boca Raton: CRC Press, Taylor & Francis Group, 2016.

[10] X. Chen and K. Wu, "Substrate Integrated Waveguide Filter: Basic Design Rules and Fundamental Structure Features," in *IEEE Microwave Magazine*, vol. 15, no. 5, pp. 108-116, July-Aug. 2014.

[11] X. Chen and K. Wu, "Substrate Integrated Waveguide Filters: Design Techniques and Structure Innovations," in *IEEE Microwave Magazine*, vol. 15, no. 6, pp. 121-133, Sept.-Oct. 2014.

[12] X. Chen and K. Wu, "Substrate Integrated Waveguide Filters: Practical Aspects and Design Considerations," in *IEEE Microwave Magazine*, vol. 15, no. 7, pp. 75-83, Nov.-Dec. 2014.

[13] A. Rhbanou, M. Sabbane and S. Bri, "Design of substrate integrated waveguide cavity bandpass filters," 2016 *5th International Conference on Multimedia Computing and Systems (ICMCS)*, Marrakech, 2016.

[14] Y. Wang, Y. Fu, Q. Liu and S. Dong, "Design of a substrate integrated waveguide bandpass filter using in microwave communication systems," 2010 *International Conference on Microwave and Millimeter Wave Technology*, Chengdu, 2010.

[15] Y. D. Parmar and S. C. Bera, "Investigation of substrate integrated waveguide filters and construction technique," 2017 *International Conference on Computing Methodologies and Communication (ICCMC)*, Erode, 2017.

[16] Feng Xu and Ke Wu, "Guided-wave and leakage characteristics of substrate integrated waveguide," in *IEEE Transactions on Microwave Theory and Techniques*, vol. 53, no. 1, pp. 66-73, Jan. 2005.

[17] J. M. George and S. Raghavan, "A design of miniaturized SIW-based band-pass cavity filter," 2017 *International Conference on Communication and Signal Processing (ICCSP)*, Chennai, 2017.

[18] M. Bozzi, A. Georgiadis and K. Wu, "Review of substrate-integrated waveguide circuits and antennas," in *IET Microwaves, Antennas & Propagation*, vol. 5, no. 8, pp. 909-920, 6 June 2011.

[19] F. Parment, A. Ghiotto, T. Vuong, J. Duchamp and K. Wu, "Low-loss air-filled Substrate Integrated Waveguide (SIW) band-pass filter with inductive posts," 2015 *European Microwave Conference (EuMC)*, Paris, 2015.

[20] B. Veadesh, S. Aswin and K. Shambavi, "Design and analysis of C-band siw directional coupler," 2017 *International conference on Microelectronic Devices, Circuits and Systems (ICMDCS)*, Vellore, 2017.

[21] M. Bozzi, L. Perregrini and K. Wu, "Modeling of Radiation, Conductor, and Dielectric Losses in SIW Components by the BI-RME Method," 2008 *European Microwave Integrated Circuit Conference*, Amsterdam, 2008.

[22] J. Li, M. Mimsyad, C. Hou, C. G. Hsu and M. Ho, "Balanced Diplexer Design Using Multi-Layered Substrate Integrated Waveguide Cavities," 2018 *48th European Microwave Conference (EuMC)*, Madrid, 2018, pp. 707-710.

[23] Z. Kordiboroujeni and J. Bornemann, "Substrate integrated waveguide diplexer with dual-mode junction cavity," 2015 *European Microwave Conference (EuMC)*, Paris, 2015.

[24] Z. Kordiboroujeni and J. Bornemann, "Mode Matching design of substrate integrated waveguide diplexers," 2013 *IEEE MTT-S International Microwave Symposium Digest (MTT)*, Seattle, WA, 2013.

[25] P. Chu, K. Zheng and F. Xu, "A planar diplexer using hybrid substrate integrated waveguide and coplanar waveguide," 2017 *IEEE 17th International Conference on Ubiquitous Wireless Broadband (ICUWB)*, Salamanca, 2017.

[26] F. Mira, J. Mateu and C. Collado, "Mechanical Tuning of Substrate Integrated Waveguide Filters," in *IEEE Transactions on Microwave Theory and Techniques*, vol. 63, no. 12, pp. 3939-3946, Dec. 2015

[27] F. Mira, J. Mateu and C. Collado, "Mechanical Tuning of Substrate Integrated Waveguide Resonators," in *IEEE Microwave and Wireless Components Letters*, vol. 22, no. 9, pp. 447-449, Sept. 2012

[28] A. Collado, F. Mira and A. Georgiadis, "Mechanically Tunable Substrate Integrated Waveguide (SIW) Cavity Based Oscillator," in *IEEE Microwave and Wireless Components Letters*, vol. 23, no. 9, pp. 489-491, Sept. 2013

[29] F. Huang, J. Zhou and W. Hong, "Ku Band Continuously Tunable Circular Cavity SIW Filter With One Parameter," in *IEEE Microwave and Wireless Components Letters*, vol. 26, no. 4, pp. 270-272, April 2016

[30] S. Adhikari, Y. Ban and K. Wu, "Magnetically Tunable Ferrite Loaded Substrate Integrated Waveguide Cavity Resonator," in IEEE Microwave and Wireless Components Letters, vol. 21, no. 3, pp. 139-141, March 2011

[31] S. Adhikari, A. Ghiotto and K. Wu, "Simultaneous Electric and Magnetic Two-Dimensionally Tuned Parameter-Agile SIW Devices," in *IEEE Transactions on Microwave Theory and Techniques*, vol. 61, no. 1, pp. 423-435, Jan. 2013

[32] V. Sekar, M. Armendariz and K. Entesari, "A 1.2–1.6-GHz Substrate-Integrated-Waveguide RF MEMS Tunable Filter," in *IEEE Transactions on Microwave Theory and Techniques*, vol. 59, no. 4, pp. 866-876, April 2011.

[33] M. Armendariz, V. Sekar and K. Entesari, "Tunable SIW bandpass filters with PIN diodes," *The 40th European Microwave Conference*, Paris, 2010.

[34] S. Sirci, J. D. Martínez and V. E. Boria, "Low-loss 3-bit tunable SIW filter with PIN diodes and integrated bias network," 2013 *European Microwave Conference*, Nuremberg, 2013.

[35] F. He, X. Chen, K. Wu and W. Hong, "Electrically tunable substrate integrated waveguide reflective cavity resonator," 2009 *Asia Pacific Microwave Conference*, Singapore, 2009.

[36] S. Sirci, J. D. Martínez, M. Taroncher and V. E. Boria, "Varactor-loaded continuously tunable SIW resonator for reconfigurable filter design," 2011 41st *European Microwave Conference*, Manchester, 2011.

[37] D. Zhao and L. Li, "A Dual-mode SIW Filter with Tunable Frequency, Reconfigurable Bandwidth and Adjustable Transmission Zero," 2018 *International Applied Computational Electromagnetics Society Symposium* - China (ACES), Beijing, China, 2018.

[38] M. Sun, J. Zhang, Z. Zheng, J. Yang, X. Zhu and R. Leng, "A 3-4.5 GHz Electrically Reconfigurable Bandpass Filter Based on Substrate Integrated Waveguide," 2019 *IEEE 6th International Symposium on Electromagnetic Compatibility (ISEMC),* Nanjing, China, 2019.

[39] M. Deng and D. Psychogiou, "Tune-All Substrate-Integrated-Waveguide (SIW) Bandpass Filters," 2019 *14th European Microwave Integrated Circuits Conference (EuMIC)*, Paris, France, 2019.

[40] E. E. Djoumessi and K. Wu, "Electronically tunable diplexer for frequency-agile transceiver front-end," 2010 *IEEE MTT-S International Microwave Symposium, Anaheim*, CA, 2010.

[41] S. Wong, F. Deng, J. Lin, Y. Wu, L. Zhu and Q. Chu, "An Independently Four-Channel Cavity Diplexer With 1.1–2.8 GHz Tunable Range," in *IEEE Microwave and Wireless Components Letters*, vol. 27, no. 8, pp. 709-711, Aug. 2017.

[42] L. Gao, T. Lin and G. M. Rebeiz, "Tunable Three-Pole Diplexer with High Selectivity and Isolation," 2018 *IEEE/MTT-S International Microwave Symposium - IMS*, Philadelphia, PA, 2018.

[43] J. Xu and Y. Zhu, "Tunable Bandpass Filter Using a Switched Tunable Diplexer Technique," in *IEEE Transactions on Industrial Electronics*, vol. 64, no. 4, pp. 3118-3126, April 2017.

[44] Y. Yang, M. Yu, Q. Wu and Y. Zeng, "Tunable Diplexer Design with Redundant Coupling," in *IEEE Transactions on Microwave Theory and Techniques*, vol. 67, no. 12, pp. 4976-4983, Dec. 2019.

[45] Z. Li, X. Tang, D. Lu and M. Yu, "Tunable Diplexer with Identical Passband and Constant Absolute Bandwidth," *in IEEE Transactions on Microwave Theory and Techniques*, vol. 68, no. 2, pp. 721-731, Feb. 2020.

[46] M. F. Hagag, M. Abu Khater, M. D. Hickle and D. Peroulis, "Tunable SIW Cavity -Based Dual-Mode Diplexers with Various Single-Ended and Balanced Ports," in *IEEE Transactions on Microwave Theory and Techniques*, vol. 66, no. 3, pp. 1238 -1248, March 2018.

[47] A. Iqbal, J. J. Tiang, C. K. Lee and B. M. Lee, "Tunable Substrate Integrated Waveguide Diplexer with High Isolation and Wide Stopband," in *IEEE Microwave and Wireless Components Letters*, vol. 29, no. 7, pp. 456-458, July 2019.

[48] B. Krishnan and S. Raghavan, "A Review on Substrate Integrated Waveguide Transitions," 2019 TEQIP III Sponsored International Conference on *Microwave Integrated Circuits, Photonics and Wireless Networks (IMICPW)*, Tiruchirappalli, India, 2019.

[49] S. Mukherjee, P. Chongder, K. V. Srivastava and A. Biswas, "Design of a broadband coaxial to substrate integrated waveguide (SIW) transition," 2013 *Asia-Pacific Microwave Conference Proceedings (APMC),* Seoul, 2013.

[50] D. Deslandes, "Design equations for tapered microstrip-to-Substrate Integrated Waveguide transitions," 2010 IEEE *MTT-S International Microwave Symposium*, Anaheim, CA, 2010.

[51] E. Miralles, H. Esteban, C. Bachiller, A. Belenguer and V. E. Boria, "Improvement for the design equations for tapered Microstrip-to-Substrate Integrated Waveguide transitions," 2011 *International Conference on Electromagnetics in Advanced Applications*, Torino, 2011.

[52] MACOM, “MAVR-011020-1411,” [Online] Available: http://www.macom.com/products/pruduct-detail/MAVR-011020-1411.